Animal Behaviour 179 (2021) 247–265

Contents lists available at ScienceDirect

Animal Behaviour

journal homepage: www.elsevier.com/locate/anbehav

Negative frequency-dependent prey selection by wolves and its implications on predator–prey dynamics

Sarah R. Hoy [a, *], Daniel R. MacNulty [b], Matthew C. Metz [c, d], Douglas W. Smith [d], Daniel R. Stahler [d], Rolf O. Peterson [a], John A. Vucetich [a]

[a] College of Forest Resources and Environmental Science, Michigan Technological University, Houghton, MI, U.S.A.
[b] Department of Wildland Resources, Utah State University, Logan, UT, U.S.A.
[c] W.A. Franke College of Forestry & Conservation, University of Montana, Missoula, MT, U.S.A.
[d] Yellowstone Wolf Project, Yellowstone Centre for Resources, Yellowstone National Park, WY, U.S.A.

ARTICLE INFO

Article history:
Received 23 December 2020
Initial acceptance 19 February 2021
Final acceptance 1 April 2021
Available online 11 August 2021
MS. number: A20-00913R

Keywords:
age structure
Alcesalces
Canis lupus
Cervuscanadensis
demographic structure
diet selection
foraging strategy
frequency-dependent selection
predator–prey dynamics
selective predation

Many species exhibit selective foraging behaviour, where consumers use a nonrandom subset of available food types. Yet little is known about how selective foraging behaviour varies with environmental conditions and the community level consequences of such selection dynamics. We examined selective foraging by wolves preying primarily on elk in Yellowstone National Park (YNP) over a 12-year period and on moose in Isle Royale National Park (IRNP) over a 47-year period. Specifically, we assessed how selection for calves and senescent adults varied with their frequency in the environment, wolf abundance and winter severity. Selection for senescent adults decreased as the relative abundance of senescent prey increased (i.e. negative frequency-dependent selection) in both study sites. In IRNP, selection for calves was also negatively frequency dependent and declined with increasing wolf abundance. These results are inconsistent with the pattern of positive frequency-dependent selection expected under the prey-switching hypothesis. These results suggest that selection is primarily driven by intraspecific differences in prey vulnerability and wolves' interest in minimizing their risk of injury, as opposed to maximizing intake rates. Lastly, we ran simulations to evaluate how predator–prey dynamics were influenced by dynamic patterns of selection, like those observed in YNP and IRNP. The simulations indicated that predators are more efficient (i.e. steeper slope of the numerical response) when selection for calves is negatively frequency dependent, which results in a lower mean abundance of prey. More importantly, predation is a stronger destabilizing force when selection for calves is negatively frequency dependent. That stronger destabilizing force is indicated by greater variability in the abundance of prey and predators, prey populations being less resilient and a steeper negative slope of the relationship between predation rate and prey population growth rate. As such, our simulation analyses suggest that some of the observed patterns of negative-frequency dependent selection may have important consequences for predator–prey dynamics.

Selective foraging behaviour is thought to have a strong, yet poorly understood, influence on community level dynamics and the stability of ecosystems (Ellis, Wiens, Rodell, & Anway, 1976). Selective foraging occurs when consumers utilize a nonrandom subset of available resource types. A resource type is considered to be 'selected for' when its relative frequency in the consumer's diet exceeds its relative frequency in the environment, and 'avoided' when its relative frequency in the diet is lower than its relative frequency in the environment. Selective predation is thought to arise from trade-offs associated with various properties of prey types, such as body size, nutritional value, energetic and temporal costs of acquiring prey and risks of injury associated with capturing and handling prey (Berger-Tal, Mukherjee, Kotler, & Brown, 2009; MacArthur & Pianka, 1966; Stephens & Krebs, 1986; Werner & Hall, 1974).

Foraging selection by predators may occur among prey species (interspecific selection) or among demographic classes within a prey species (intraspecific selection; Reimer, Brown, Beltaos-Kerr, & de Vries, 2019). For example, predators often exhibit strong selection for juveniles because they are easier to capture, even though their nutritional value is lower than adults, due to their smaller

* Corresponding author.
E-mail address: sarah.r.hoy@gmail.com (S. R. Hoy).

https://doi.org/10.1016/j.anbehav.2021.06.025
0003-3472/

body size (Hoy et al., 2015; Metz, Smith, Vucetich, Stahler, & Peterson, 2012; Wright, Peterson, Smith, & Lemke, 2006). Intraspecific selection can also occur among adult prey because of differences in age, size, conspicuousness, behaviour and body condition – or any trait that makes prey easier for predators to detect and catch (Hoy et al., 2015; Magnhagen, 1991; Temple, 1987).

Selective foraging is a dynamic process that can be influenced by changes in the relative frequency of prey types in the environment, because such changes may influence predator search time and where predators search for prey (Murdoch, 1969; Oaten & Murdoch, 1975). Positive frequency-dependent selection occurs when the strength of selection for a particular resource type increases with its relative abundance in the environment. This foraging strategy is associated with predators switching to an alternative prey species when the primary prey species becomes rare (i.e. the prey-switching hypothesis: Garrott, Bruggeman, Becker, Kalinowski, & White, 2007; O'Donoghue et al., 1998; Oaten & Murdoch, 1975) and is thought to maximize the foraging efficiency and intake rate of predators (Hughes & Croy, 1993; Murdoch, 1969; Stephens & Krebs, 1986). Negative frequency-dependent selection occurs when the strength of selection for a resource type is greatest when its relatively rare in the environment (Edenius, Ericsson, & Näslund, 2002; Hoy et al., 2019). Negative frequency dependence can arise when prey types differ in terms of vulnerability or their potential for injuring the predator (Tallian et al., 2017). Therefore, it may involve predators trading off a potentially higher intake rate for a lower risk of injury. Consequently, frequency-dependent prey selection is likely to influence kill rates and thereby the growth of the predator population.

The direction, strength and linearity of frequency-dependent selection exhibited by consumers can influence the stability of communities (Garrott et al., 2007; Hoy et al., 2019). For example, when predators (living with multiple prey species) exhibit positive frequency dependence it tends to favour stability and coexistence among prey species by regulating the abundance of common species (Murdoch & Oaten, 1975; Oaten & Murdoch, 1975). Conversely, negative frequency dependence may be destabilizing and disfavour coexistence if rare species are more likely to become extinct. Although a few studies have examined community level consequences of frequency-dependent selection among prey species, very little is known about the population level or community level consequences of selection among different classes of individuals within a species (but see Boukal, Berec, & Křivan, 2008; Reimer et al., 2019).

Vital rates and reproductive value vary importantly with age and sex for many species (Nussey, Froy, Lemaitre, Gaillard, & Austad, 2013). Therefore, the demographic composition (sex and age) of prey killed can be an important determinant of the overall impact of predation on prey populations (Boukal et al., 2008; Gervasi et al., 2012; Hoy et al., 2015). For example, simulations indicate that reductions in prey (tawny owl, *Strix aluco*) population size can be 50% greater if predators (northern goshawk, *Accipiter gentilis*) selectively prey on prime-aged adults (with high reproductive values) compared to when they prey on juveniles and senescent adults (with lower reproductive values; Hoy et al., 2015). Given that the demographic structure of prey populations can fluctuate considerably over time (Hoy et al., 2020), those changes may have an important, but underappreciated, effect on selective foraging and thus predator–prey dynamics.

Empirical assessments of the environmental processes shaping intraspecific prey selection are rare, despite the number of studies documenting predator preferences for certain demographic classes of prey (e.g. Hoy et al., 2015; Wright et al., 2006). The paucity of such studies likely stems from the logistical difficulties of gathering the data necessary for assessing frequency-dependent selection (Hassell, 2000). Here we examined temporal variation in intraspecific prey selection by grey wolves, *Canis lupus*, in two study systems, the Northern Range of Yellowstone National Park (YNP) where the primary prey is elk, *Cervus canadensis*, and Isle Royale National Park (IRNP) where the primary prey is moose, *Alces alces*. We quantified the strength of selection for demographic classes of elk and moose using the Manly–Chesson index, denoted α, which is calculated from annual estimates of the relative frequency of different demographic classes in predator diets (hereafter, dietary frequency) and annual estimates of the relative frequency of different demographic classes in the prey population (hereafter, environmental frequency). Although there are several indices of selection that quantify a consumer's use in relation to environmental availability, we used the Manly–Chesson index because it allows for a direct connection between foraging behaviour and predator–prey dynamics (as illustrated in equation 2; see below). For emphasis, we focus exclusively on selection for different demographic classes of the primary prey species (elk in YNP and moose in IRNP) and not on selection among different species of prey as that has been the focus of prior research (e.g. Tallian et al., 2017).

We estimated values of α each year in YNP during 1998–2009 and in IRNP during 1959–2007. We examined whether values of α were frequency dependent and whether they covaried with predator density (an index of intraspecific competition) and winter severity because both of these factors are known to affect other aspects of predator foraging behaviour (e.g. kill rates and capture success: Post, Peterson, Stenseth, & McLaren, 1999; Vucetich, Peterson, & Schaefer, 2002; Wilmers et al., 2020). It is plausible that predators may become less selective as predator density, hence competition for food, increases (e.g. Barnard & Brown, 1981). It is also plausible that wolves may be less selective during severe winters because winter severity can influence both the nutritional condition and mobility of prey, thereby influencing their vulnerability to predation (Mech, McRoberts, Peterson, & Page, 1987; Parker, Robbins, & Hanley, 1984; Post et al., 1999). For example, there is some evidence that predation on adult female elk may increase in years with harsh winters because deep snow 'levels the playing field' by making all animals highly vulnerable to predation (Wilmers et al., 2020). To clarify, the aspiration of this analysis is not to develop a complete model of causal influences on selection; rather, we aim to assess whether selection is importantly associated with a small set of factors for which there is strong a priori reason to think there is an association. We then built simulation models to better understand how selective foraging dynamics like those observed in YNP and IRNP are likely to affect population dynamics of the predator and prey. For example, we tested hypotheses pertaining to whether the selection dynamics observed in our two study systems were likely to have a stabilizing or destabilizing influence on predator–prey dynamics.

METHODS

Study Systems

One of our study systems is the Northern Range of YNP (995 km^2), which is located in the central Rocky Mountains of North America (44 °N, 110 °W). The wolf–elk system has been intensively studied since wolves were reintroduced during 1995–1997 (MacNulty et al., 2020). The climate is characterized by long, cold winters and short, cool summers (Houston, 1982). At any

time during the study period, approximately 35–40% of wolves were outfitted with radiocollars, generally including at least one collared individual in each pack (Smith & Bangs, 2009). Wolf abundance was estimated each March–April from counts of adults and 11-month-old pups. Wolf abundance fluctuated between 40 and 106 wolves, with an average pack size of 10–11 wolves, during the study period (Smith & Bangs, 2009). Elk are the main prey for wolves in the Northern Range of YNP, comprising an average of 85–96% of their kills, with the remainder comprising a range of other ungulate species (Metz et al., 2012).

The other study system is IRNP, an island (544 km^2) located in Lake Superior, North America (48 °N, 89 °W), where populations of wolves and moose have been continuously studied since 1959 (Peterson, Vucetich, Bump, & Smith, 2014). The climate is characterized by warm summers and cold, snowy winters. Wolf abundance was estimated annually by aerial observation each January–February from a fixed-wing aircraft (Peterson & Page, 1988). Those observations were aided by most packs having at least one collared wolf during most years. The wolf population fluctuated between 12 and 50 wolves, with an average pack size of eight wolves, during the study period (Peterson, Thomas, Thurber, Vucetich, & Waite, 1998). Moose are the primary prey for wolves, comprising an average of 90% of their kills, with the remainder mostly composed of beaver, *Castor canadensis* (Peterson et al., 1998).

Data Collection

Each year we conducted intensive aerial and ground surveys in YNP (1995–2015) and IRNP (1959–2015) to locate carcasses of dead elk and moose (Metz et al., 2012; Montgomery, Vucetich, Roloff, Bump, & Peterson, 2014). These surveys were done consistently and at similar times during each year of the study. In particular, intensive surveys were conducted each year from mid-January to late-February in IRNP and in both early winter (November–December) and late winter (March) in YNP. Survey efforts were most intensive during winter because wolf tracks left in the snow and the lack of green vegetation allow for more reliable detection of carcasses. We necropsied carcasses to determine the individual's sex and age at death. Necropsies also included inferring the cause of death from field signs, such as blood on trees, signs of a chase as indicated by tracks, hair and blood in the snow and signs of struggle including broken branches (Metz et al., 2012; Montgomery et al., 2014). Elk and moose died from various causes, primarily predation, starvation and accidents. We estimated age at death for calves and yearlings through tooth eruption patterns and for adults by counting cementum lines of teeth (Haagenrud, 1978; Peterson, 1977; Rolandsen et al., 2008). We determined sex primarily on the basis of the individual's skull, specifically the presence of antlers or pedicles. In some cases, typically with calves, the skull was not recovered, or too damaged to determine the individual's sex. Overall, we determined the sex of 96% ($N = 1684$) of adult elk and 7% ($N = 1053$) of elk calves killed by wolves during 1995–2015. We also determined the sex of 95% ($N = 765$) of adult moose and 33% ($N = 409$) of moose calves killed by wolves during 1959–2015. Calves less than 6 months (elk) or 8 months (moose) of age were excluded from estimates of dietary frequency and environmental frequency. We did so because their carcasses are frequently killed and eaten without ever being detected and because these individuals died before they could be included in prey population estimates. Consequently, the assessment of selection presented here is properly considered selection for recruited calves. Hereafter we use the term 'recruited calves' to refer to elk aged 6–12 months old and moose aged 8–12 months old.

Dietary Frequency

To estimate dietary frequency, we filtered our necropsy database such that it only included moose and elk that were killed by wolves, then assigned each dead ungulate to a specific age/sex class. For elk, we considered five classes: recruited calves (6–12 months), prime-aged males (1–5 years), prime-aged females (1–12 years), senescent males (≥6 years) and senescent females (≥13 years). For moose, we considered three age classes: recruited calves (8–12 months), prime-aged adults (males and females 1–9 years) and senescent adults (≥10 years). The age ranges for classifying individuals as prime-aged or senescent were based on species-specific relationships between age and survival (Appendix 1, Fig. A1), and represent the same demographic classes used in Hoy et al. (2020). We pooled sexes of calves for elk and moose because most calf carcasses could not be sexed. We pooled sexes of adult moose because sex-specific estimates of environmental frequency were not available for this population (see below). We then estimated the annual proportion of kills belonging to each age class for each study site.

Environmental Frequency

We obtained annual estimates of the relative frequencies of each age/sex class in each prey population from Hoy et al. (2020), who estimated age structure using reconstruction analysis (Fryxell et al., 1999; Gove, Skalski, Zager, & Townsend, 2002; Solberg, Sæther, Strand, & Loison, 1999). That approach involved creating a database of year of death and age at death for individuals in each population and calculating the minimum number of individuals alive in each age class, every year. These year-specific age structures were estimated from 13 211 elk that died during 1995–2015 and from 2779 moose that died during 1959–2015. Sample size was large enough to allow for calculating sex-specific estimates of age structure for the elk population but not for the moose population. Overall, estimates of age structure were available for the elk population each year during 1995–2009 and for the moose population each year during 1959–2007.

Estimating Selection for Demographic Classes

We estimated wolves' selection for each demographic class of prey using the Manly–Chesson selection index, denoted α, which quantifies dietary frequency in relationship to environmental frequency (Chesson, 1978, 1983; Manly, 1974). Specifically, α is a relative measure of selection, which is calculated as:

$$\alpha_i = \frac{r_i / e_i}{\sum_{i=1}^{m} r_i / e_i} \quad (1)$$

where r_i is the proportion of prey item i in the diet (i.e. dietary frequency), e_i is the proportion of prey item i in the environment (environmental frequency) and m represents the number of prey types in the environment, where $m = 5$ for YNP and $m = 3$ for IRNP. Values of α_i range from 0 (complete avoidance) to 1 (strongest possible selection). The probability of a predator encountering a specific prey type is assumed to be proportional to its environmental frequency. Additionally, α is also related to the attack rate in the functional response of a consumer resource model (Chesson, 1978). We could not generate annual estimates of α_i for YNP after 2009 or for IRNP after 2007, because estimates of the age structure of elk and moose populations (hence estimates of e_i) were not available (Hoy et al., 2020). For YNP, we did not analyse α_i prior to 1998 because ongoing reintroductions of wolves might have influenced wolf foraging behaviour. Temporal

variation in dietary frequency, environmental frequency and selection for each demographic class of elk and moose is depicted in Fig. A2 in Appendix 1.

Statistical Analysis

Temporal variation in selectivity

Following Hoy et al. (2019), we logit-transformed the response variable α_i (because α_i is constrained between 0 and 1) and used regression models to assess whether it varied in response to the predictor variables: environmental frequency, wolf abundance and an index of winter severity in R v.4.0.1 (R Core Development Team, 2015). Prior research indicated that the North Atlantic Oscillation (NAO), a large-scale atmospheric condition, is a better indicator of winter severity than locally measured indicators for regions that are influence by NAO, such as IRNP (Hallet et al., 2004; Vucetich & Peterson, 2004). We obtained the mean NAO index during winter (December–March) from the National Center for Atmospheric Research (Hurrell, 1995). Because NAO does not influence YNP, we used estimates of the snow water equivalent (SWE) for the Northern Range as an index of winter severity. SWE quantifies the water content of snowpack and therefore approximates the energetic cost of elk locomotion (Wockner, Singer, Coughenour, & Farnes, 2002). Furthermore, SWE is a commonly used indicator of winter severity for ungulates in western North America (Wilmers et al., 2020). We did not include pack size as a predictor of selection because we could not always determine which packs killed individual prey. Moreover, the success of wolves hunting prey such as adult elk does not improve beyond wolf group sizes of four (MacNulty, Smith, Mech, Vucetich, & Packer, 2012), and the mean annual pack size observed in both study systems exceeded that threshold.

We focused the analysis on assessing selection (α) for recruited calves and senescent adults. We refrained from assessing selection for prime-aged individuals because a set of α_i values has one less degree of freedom than there are categories of i due to the constraint of α_i values summing to 1. We assessed the performance of regression models on the basis of R^2 and Akaike's information criterion corrected for small sample size (AICc; Burnham & Anderson, 2002). The R^2 values presented below describe the proportion of variance in the logit-transformed response variable for selection ($\text{logit}(\alpha_i)$) explained by each model. We calculated ΔAICc, which is the AICc for the model of interest minus the smallest AICc for the set of models being considered. By definition, the best model has a ΔAICc of zero. Models with $\Delta\text{AICc} > 2$ units of the best model are generally considered to be inferior, whereas models with a $\Delta\text{AICc} < 2$ are generally considered to have performed equivalently and are therefore worthy of consideration.

We built a univariate model for each predictor and then used a stepwise selection procedure to identify whether models with additional predictors were more parsimonious. We also evaluated two-way interaction terms between significant main effects when included in the same model. While a notable set of studies – mostly focussed on Cox proportional hazards models – assess the appropriate number of observations required for each predictor variable, those studies offer a wide range of appropriate ratios, from 50:1 to 5:1 (Austin & Steyerberg, 2015; Vittinghoff & McCulloch, 2007). These studies were also intended to guide the design of experiments, not the analysis of already-collected, nonexperimental data. Consequently, although we expect the YNP data to be too small to support more than one predictor, we let AIC guide judgments about possible overparameterization. Lastly, it is relevant to note that models including the predictor frequency involve statistical dependencies because our index of selectivity is estimated from environmental frequency. Such statistical dependencies are common and intrinsic to assessments of some basic ecological relationships, most notably assessments of density-dependent population growth and ratio-dependent functional responses. More importantly, these statistical dependencies do not lead to biased inferences about whether selection is positively frequency dependent, negatively frequency dependent or independent of frequency (see Appendix 1, Figs A3-A7).

Simulations

We ran simulations to better understand how different patterns of frequency-dependent selection influence predator–prey dynamics. More specifically, we built predator–prey models that accounted for the dynamic patterns of selective predation like those observed in YNP and IRNP (see Results) and also a reference model where the strength of selection remained constant over time (constant model). This predator–prey model is a pair of difference equations where ungulate demography (in the absence of predation) is determined by a 3×3 transition matrix, representing three basic life-history stages (recruited calves, prime-aged, senescent) of a generic large ungulate species. Ungulate recruitment was density dependent and influenced by environmental stochasticity (for details see Appendix 2, equation A2, equation A3, Fig. A8).

Losses to predation for each prey stage class were calculated as predator abundance times the per capita kill rate for that stage. The predators' per capita kill rate follows a type II ratio-dependent functional response, modified to account for α (Chan et al., 2017):

$$x_i = (\alpha_i z_i n_i)/(P + \alpha_i z_i h_i n_i) \quad (2)$$

where i is an index for prey stage, x is the number of prey killed per predator per unit of time, z is the attack rate, n is the number of individuals in that prey stage class, P is the total number of predators and h is handling time. Ratio dependency is justified by empirical assessments of both study populations (Becker et al., 2009; Vucetich et al., 2002). The per capita growth rate of the predator population is calculated as a linear function of the total per capita kill rate, summed across the three prey stages and adjusted to account for the smaller body size of calves. We parameterized these predator–prey models using empirically derived estimates from our study systems (see Appendix 2 for details).

We analysed the output of the simulations based on the idea that predation dynamics are largely shaped by four relationships: functional response, numerical response and two relationships involving predation rate. The first of the relationships involving predation rate is between prey abundance (abscissa) and predation rate (ordinate), which may be considered a partial explanation for what causes predation rate to fluctuate over time. The second is the relationship between predation rate (abscissa) and the per capita growth rate of the prey population (ordinate), which may be considered a partial account for the consequences of fluctuating predation rate.

We observed differences in those four relationships among three models, one model representing frequency-dependent selection like that observed in YNP (see Results, Fig. 2), another model representing frequency-dependent selection like that observed in IRNP (see Results, Fig. 3) and a reference model where selection was constant over time (see Appendix 2 for details on parameterization of frequency-dependent selection). We also conducted sensitivity analysis to determine whether the results remained consistent across a wide range of parameter values. To summarize, the sensitivity analysis involved systematically varying a subset of five parameters: the attack rate in the functional response (equation A6), the slope and intercept of the numerical response (equation A7) and the strength and shape of density-

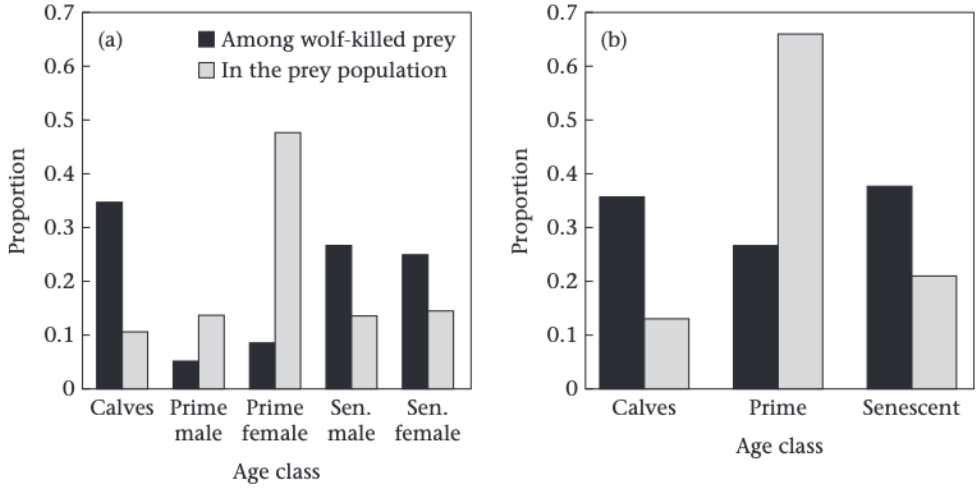

Figure 1. Differences in the relative use and frequency of different demographic classes of prey in the environment for wolves (a) preying on elk in Yellowstone National Park during 1998–2009 and (b) preying on moose in Isle Royale National Park during 1959–2007. Black bars indicate the demographic composition of wolf-killed elk and moose, averaged across years. Grey bars indicate the proportion of the prey populations belonging to each demographic class in each prey population, averaged across years. For elk, we considered five age classes: recruited calves (6–12 months), prime-aged males (1–5 years), prime-aged females (1–12 years), senescent (sen.) males (>6 years) and sen. Females (>13 years). For moose, we considered three age classes: recruited calves (8–12 months), prime-aged adults (males and females 1–9 years) and senescent adults (>10 years).

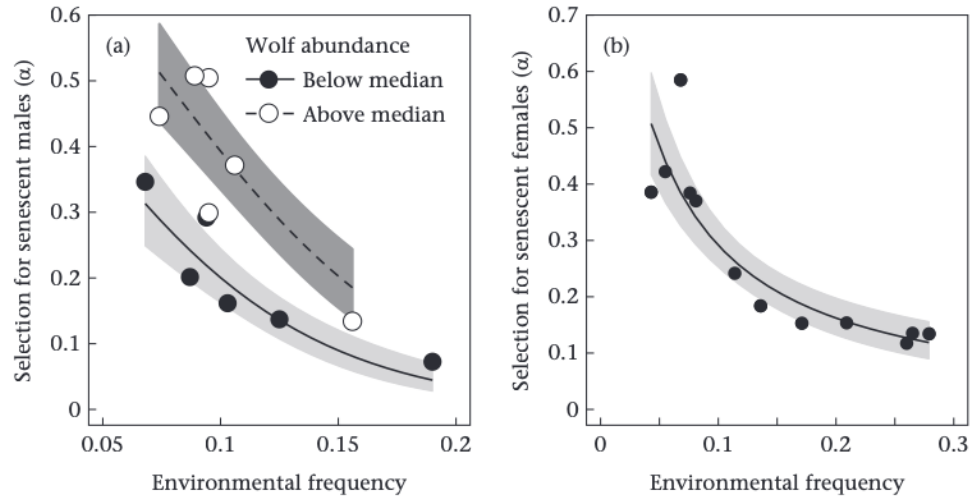

Figure 2. Negative frequency-dependent selection for (a) senescent male elk and (b) senescent female elk by grey wolves in the Northern Range of Yellowstone National Park during 1998–2009. Circles are annual estimates of prey selection (α in equation 1). In (a), the solid and dashed lines are fitted values predicted from the frequency and wolf model in Table 1, when wolf abundance was fixed at the 15th and 85th percentile, and shaded grey areas indicate 95% confidence intervals (CIs). In (b), the solid line and grey shaded area represent fitted values and 95% CIs predicted from the frequency model in Table 1. Environmental frequency is the proportion of the prey population composed of each age class.

dependent recruitment for the prey population (equation A2, Fig. A8). Each parameter was varied, one at a time, by plus and minus 20% of the baseline level. That approach for conducting sensitivity analysis is similar to Hoy et al. (2019). Each combination of parameter settings was run for 10 replicates, yielding a total of 110 replicate simulations: one set of 10 replicates with all parameters set at baseline values, five sets of 10 replicates where one of the five parameters was adjusted downward and five sets of 10 replicates where one of the five parameters was adjusted upward. Each replicate was run over 200 years, but we discarded the first 50 years as burn-in.

Lastly, we also performed a separate simulation analysis with our three models to estimate how quickly the prey population returned to equilibrium (in the absence of stochasticity) after it was perturbed by a large, exogenous force resulting in a 90% reduction in abundance. To clarify, the equilibrium is the abundance value that the population converges to in the absence of stochasticity. The speed at which the prey population recovers can provide important insights about the resilience of the system, with longer return times indicating lower resilience (Pimm, 1991). Differences in return times among the three models can be interpreted as a measure of the extent to which each pattern of selective predation is capable of slowing down the potential growth of prey population and an indication of the extent that predation is a destabilizing force. Although a decline of 90% may seem extreme, such declines have been observed for several ungulate populations in response to disease or extreme weather events, such as drought or severe winter (see Table 1 in Young, 1994). For example, several populations of bighorn sheep, *Ovis canadensis*, were observed to decline by over 85% (Stelfox, 1971; Uhazy, Holmes, & Stelfox, 1973), and the Isle Royale moose population declined by over 65% following a severe winter in 1996 (Vucetich & Peterson, 2004). We

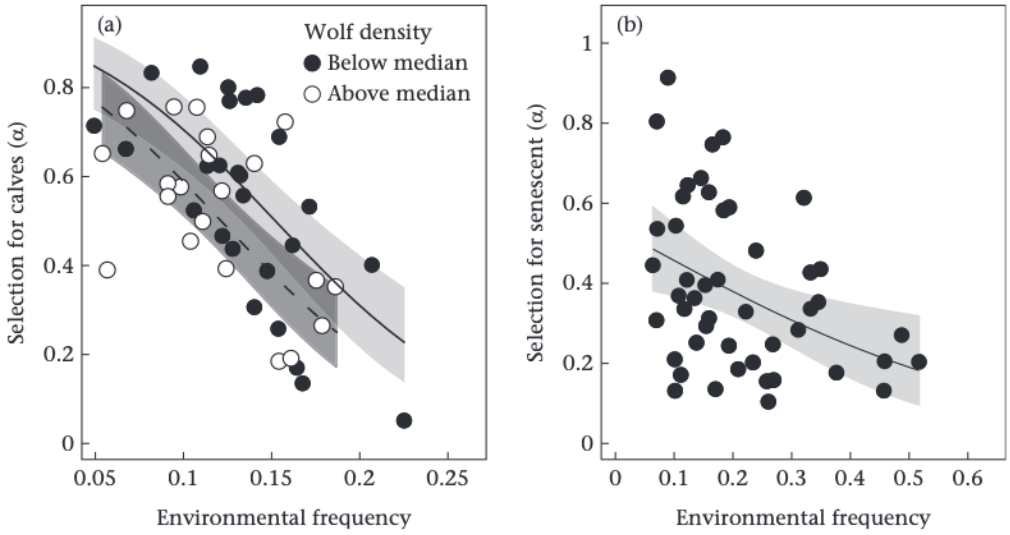

Figure 3. Negative frequency-dependent selection for (a) recruited moose calves and (b) senescent moose by wolves in Isle Royale National Park during 1959–2007. Circles are annual estimates of prey selection (α in equation 1). In (a), the solid and dashed lines are predicted values from the frequency and wolf model in Table 2, when wolf abundance was fixed at the 15th and 85th percentile. Grey areas indicate 95% confidence intervals derived from the best performing model in Table 2. Environmental frequency is the proportion of the prey population composed of each age class.

also observed an overall decline in population size of 93% for the segment of the northern Yellowstone elk population that winters inside the park, but over a longer time period, 1995–2017 (Figure 14.7 in MacNulty et al., 2020).

In summary, we used simulations to assess the consequences of three different patterns of selective predation for four different relationships shaping predator–prey dynamics and the resiliency of the prey population. The overall purpose of these simulations was to assess whether the empirically observed patterns of selective foraging are ecologically relevant for understanding predator–prey dynamics.

RESULTS

A graphical comparison of overall (time-averaged) frequencies of diet composition and environmental composition (Fig. 1), indicated that wolves preying on elk in YNP exhibited strong selection for recruited calves, weaker selection for senescent males and females and strong avoidance of prime-aged adults, especially prime-aged females (Fig. 1a). Wolves preying on moose in IRNP exhibited a similar pattern, with strong selection for recruited calves, weaker selection for senescent moose and avoidance of prime-aged moose (Fig. 1b).

In YNP, selection for recruited calves remained high throughout the study period and frequency was not a useful predictor of selection for elk calves ($P = 0.56$; Table 1). The best predictor of selection for elk calves was wolf abundance, which explained 34% of the variation in α ($P - 4.6 \times 10^{-2}$). However, the wolf abundance model was within 1.4 AICc units of the null model (Table 1). Selection for senescent male elk was most parsimoniously predicted by environmental frequency ($P = 4.19 \times 10^{-5}$) and wolf abundance ($P = 8.57 \times 10^{-4}$) with selection declining as the relative frequency of senescent males increased in the elk population (i.e. negative frequency dependence) and being greater in years when wolf abundance was high (Fig. 2a). The model with both environmental frequency and wolf abundance as predictors explained 90% of the variance in α, and the second-best model had a ΔAIC > 10 (Table 1). The data did not support a

Table 1
Performance of models predicting foraging selection by grey wolves for demographic classes of their primary prey, elk, in the Northern Range of Yellowstone National Park during 1998–2009

Response variable	Predictor variable	Coefficient	SE	ΔAICc	R^2
Selection for recruited calves, logit(α_c)	Null	–	–	1.4	–
	Frequency	−2.49	4.05	4.6	0.04
	Winter	−0.09	0.11	4.2	0.07
	Wolf	**−0.01**	**<0.01**	**0**	**0.34**
Selection for senescent males, logit(α_{sm})	Null	–	–	18.9	–
	Frequency	−18.63	4.60	10.9	0.62
	Winter	0.07	0.34	22.5	<0.01
	Wolf	0.02	0.01	18.7	0.27
	Frequency, wolf	**-18.68, 0.02**	**2.53, <0.01**	**0**	**0.90**
Selection for senescent females, logit(α_{sf})	Null	–	–	17.8	–
	Frequency[a]	**−1.09**	**0.15**	**0**	**0.83**
	Winter	0.09	0.32	21.4	0.01
	Wolf	−0.02	0.01	19.0	0.19

Recruited calves refers to elk aged 6–12 months, senescent males refers to elk ≥6 years, and senescent females refers to elk ≥13 years. The response variable was logit transformed and the candidate predictor variables were frequency (relative frequency of that demographic class in the environment), winter (winter severity indexed by the snow water equivalent), wolf (wolf abundance). The best-fitting model has an ΔAICc of zero and is shown in bold.

[a] Indicates that the relationship was best described by log transforming the predictor variable.

model including an interaction between environmental frequency and wolf abundance, which is not surprising given the small number of observations for the YNP data set. Despite the small sample size, *P* values and AIC values offered no reason to think that the bivariate (frequency and wolf) model was overparameterized. Nevertheless, inspecting the univariate models is useful if there are concerns about overparameterization. The univariate environmental frequency model explained 62% of the variation in α for senescent males and performed substantially better than the null model ($P = 2.27 \times 10^{-3}$, ΔAICc = 8.0). Although the univariate wolf abundance model explained 27% of the variation in α, it performed similarly to the null model ($P = 0.08$, ΔAICc = 0.2; Table 1). Selection for senescent female elk was best predicted by environmental frequency, which explained 83% of the variation in α ($P = 8.39 \times 10^{-5}$; Table 1), with selection declining as the relative frequency of senescent females increased in the elk population (i.e. negative frequency dependence; Fig. 2b). Winter severity was not a useful predictor of selection for any age class of elk insomuch as it explained very little variation in selectivity (Table 1).

In IRNP, selection for recruited calves declined as the relative frequency of calves increased in the moose population and to a lesser extent as wolf abundance increased (Fig. 3a). More specifically, the most parsimonious model of selection for moose calves included environmental frequency ($P = 1.64 \times 10^{-6}$) and wolf abundance ($P - 0.03$) and explained 42% of the interannual variation in α (Table 2, Fig. 3a). There was weaker evidence of a decline in selection for senescent moose as the relative frequency of senescent adults increased in the moose population (i.e. negative frequency dependence; Fig. 3b) as frequency explained only 15% of the variance in α ($P - 0.01$; Table 2). Wolf abundance was a poor predictor of selection for senescent moose ($P = 0.78$; Table 2). As with elk, winter severity was not a useful predictor of selection for any age class insomuch as models including winter explained very little variation in selectivity (Table 2). Although selection for recruited calves and senescent moose tended to decline with environmental frequency, there was much unexplained variation in selectivity among years (Fig. 3), some of which could be due to changes in the absolute number of moose or other climatic factors.

The simulation results (Fig. 4) indicated that the four basic relationships that we examined were more strongly affected by negatively frequency-dependent selection for calves (as observed in IRNP) than for senescent adults (as observed in YNP). For example, the slopes of the numerical response (Fig. 4b) and the relationship between predation rate and prey population growth rates (Fig. 4d) were substantially steeper when selection for calves was negatively frequency dependent. More importantly, the influence of negative frequency-dependent selection for calves on those relationships also resulted in lower prey abundance (Fig. 5a) and affected aspects of stability, including increased fluctuations in predator and prey abundances (Fig. 5b and c) and longer return times (Fig. 6). For example, the prey population took three times as long to return to its equilibrium value when selection for calves was negatively frequency dependent, as opposed to when it remained constant (Fig. 6). Lastly, it is relevant to note that neither the predator nor the prey populations went extinct during the simulations.

DISCUSSION

Wolves selected for recruited calves and senescent adults at both study sites (Fig. 1). This pattern is consistent with prior work (Metz et al., 2012; Wright et al., 2006) and is widely accepted to result from calves being smaller and senescent individuals being in poorer condition, which makes those age classes easier and less dangerous to kill. This study advances insights about those generally accepted patterns to show that selection for vulnerable demographic classes of prey is strongly negatively frequency dependent (Figs 2, 3) and demonstrates how frequency-dependent selection can have important consequences for predator–prey dynamics (Figs 4–6).

The dynamic patterns of selection observed here (Figs 2, 3) are not consistent with the positive frequency-dependent selection predicted by the prey-switching hypothesis, a basic principle of foraging theory (Garrott et al., 2007; O'Donoghue et al., 1998; Oaten & Murdoch, 1975). More precisely, we observed that the strength of selection for recruited calves was independent of the relative frequency of calves for elk in YNP, and the strength of selection for recruited calves declined as the relative frequency of calves increased for moose in IRNP (Tables 1, 2). Selection for senescent adults also declined as their relative frequency increased at both study sites, but to a lesser extent in IRNP (Figs 2, 3c). Declines in the relative abundance of calves or senescent adults were not accompanied by an increase in predation on prime-aged adults in either study site, providing additional evidence for the absence of prey-switching behaviour (see Appendix 3). The negative frequency dependence that we observed most likely arose because it is beneficial for predators to continue searching for the most vulnerable prey age classes (calves and senescent adults), even when they are relatively rare, rather than to risk attacking the more abundant and difficult prime-age class. Therefore, Fig. 2 (and to a lesser extent Fig. 3b) suggest that even subtle differences in prey vulnerability, such as the difference between senescent and prime-aged adults, may prevent the prey-switching behaviour that is expected to occur between (as opposed to within) species of mammalian prey (but see Reimer et al., 2019). More importantly, these results (Figs 2, 3) are more consistent with selection being primarily driven by intrinsic differences in prey vulnerability and

Table 2
Performance of models predicting foraging selection by wolves for demographic classes of their primary prey, moose, in Isle Royale National Park during 1959–2007

Response variable	Predictor variable	Coefficient	SE	ΔAICc	R^2
Selection for recruited calves, logit(α_c)	Null	–	–	20.4	–
	Frequency	−15.02	3.05	2.4	0.35
	Winter	0.12	0.06	19.2	0.07
	Wolf	−0.01	0.02	22.4	0.01
	Frequency, wolf	**−16.95; −0.03**	**3.06; 0.01**	**0**	**0.42**
	Frequency, wolf, Frequency:wolf	−28.38; −0.08; 0.48	11.75; 0.05; 0.48	1.4	0.43
Selection for senescent adults, logit(α_s)	Null	–	–	5.1	–
	Frequency	**−3.19**	**1.15**	**0**	**0.15**
	Winter	−0.11	0.06	4.3	0.06
	Wolf	−0.005	0.02	7.3	<0.01

Recruited calves refers to moose aged 8–12 months, and senescent adults refers to moose >10 years old. The best-fitting model has an ΔAICc of zero and is shown in bold. Other details are as in Table 1, except that here winter is winter severity indexed by the North Atlantic Oscillation index.

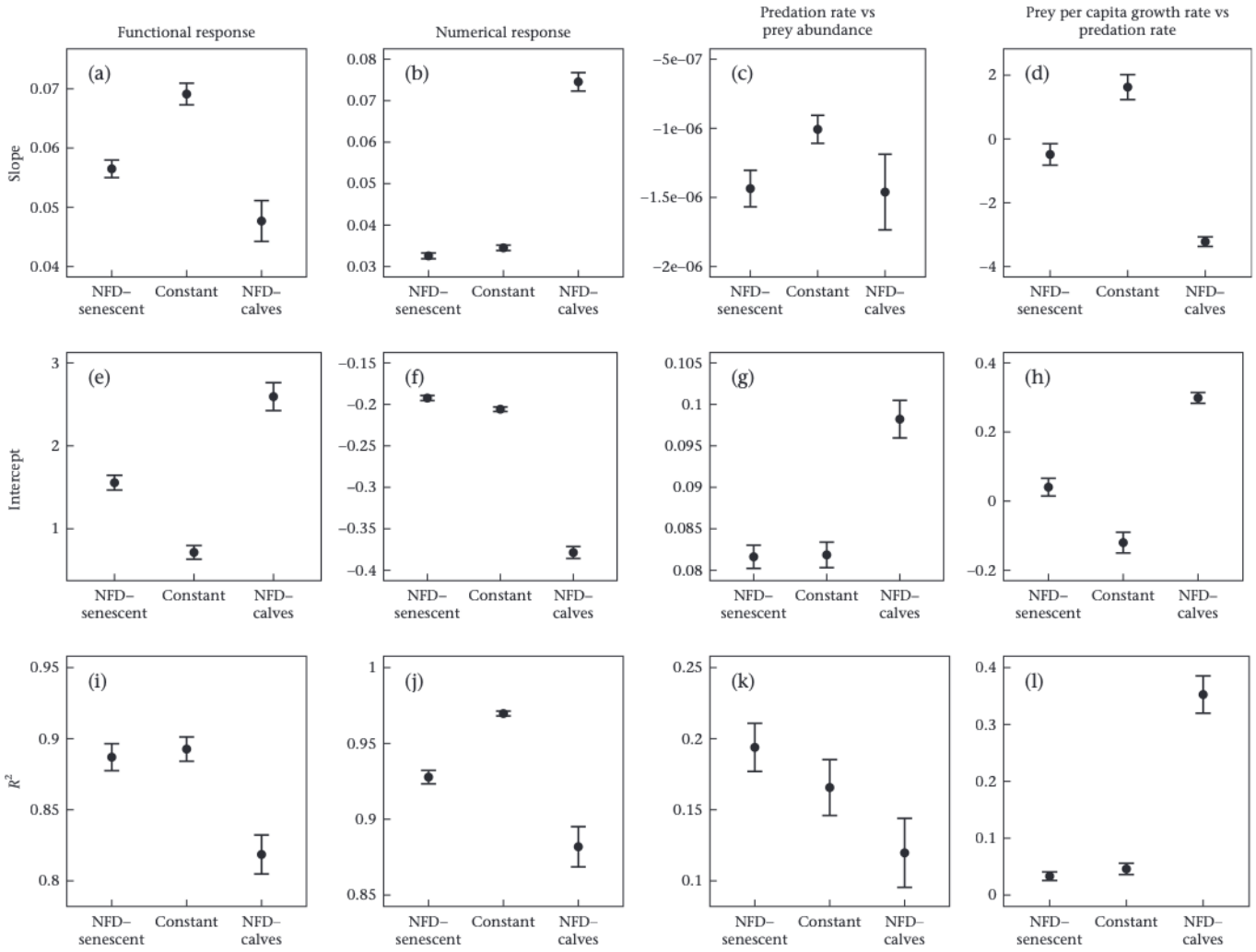

Figure 4. Results of simulations assessing the influence of frequency-dependent selective predation on different age classes of prey on four predation relationships, where each column of graphs represents a different relationship and each row represents a different aspect of each relationship. Each circle and pair of bars is a mean and 95% confidence interval for 110 replicates, representing a range of parameter values (see Methods). The three models being compared are as follows: constant, where predators' preferences were constant over time and approximated by the pattern shown in Fig. 1a; NFD-senescent, where selection for senescent adults was strongly negative-frequency dependent and selection for juvenile prey was strong but remained constant (approximating the patterns observed in Yellowstone; Fig. 2); NFD-calves model, where negative-frequency dependent selection was strong for juveniles and weak for senescent adults (approximating the patterns observed in Isle Royale; Fig. 3, see also Fig. A6) The four relationships (indicated by columns) are as follows: functional response, which is the per capita kill rate as a function of the ratio of prey to predators; numerical response, which is the per capita growth rate of the predator population as a function of per capita kill rate; predation rate as a function of prey density; and per capita prey growth rate as a function of predation rate.

the predators' interest to minimize the risk of injury, as opposed to maximizing intake rate (Mukherjee & Heithaus, 2013; Tallian et al., 2017).

The negative frequency-dependent selection that we observed (Figs 2, 3) implies that wolves may spend more time searching for prey during years when vulnerable classes of prey are rarer. Because search time is a basic constituent of per capita kill rate, our observations suggest that kill rate is also likely to be lower when calves and senescent adults are relatively rare. Therefore, our work importantly complements and synthesizes earlier studies suggesting that kill rate is influenced by the overall abundance of prey (Vucetich et al., 2002), the age structure of prey populations (Sand et al., 2012) and the proportion of the diet composed of calves (Metz et al., 2012). Although detailed assessments of both kill rate and predation rate (proportion of the prey population killed by predators) exist for both systems (Metz et al., 2012; Vucetich et al., 2002, 2011), it is not yet clear whether patterns of frequency-dependent selection can be inferred or predicted from temporal variation in kill rate, predation rate or the shape of the predator's functional response. Therefore, worthwhile insights are likely to be gained by future studies evaluating these topics. Other valuable insights may also be gained by studies assessing the role of satiation in shaping selection dynamics given that a predator's functional response and intake rates are importantly shaped by satiation.

Foraging selection is generally thought to be influenced by the degree of spatial segregation among prey types (Hubbard, Cook, Glover, & Greenwood, 1982). For example, if prey types occupy different kinds of habitat, then predators will only be able to search for one kind of prey at a time. That mechanism may cause the predator to switch from hunting in habitats preferred by its primary prey to habitats preferred by its secondary prey when the abundance of its primary prey drops below a certain threshold. In both our study systems, wolves routinely encounter different prey types (of the same species and different species) in the same habitat. An adequate understanding of the role that spatial segregation plays in shaping frequency-dependent foraging selection

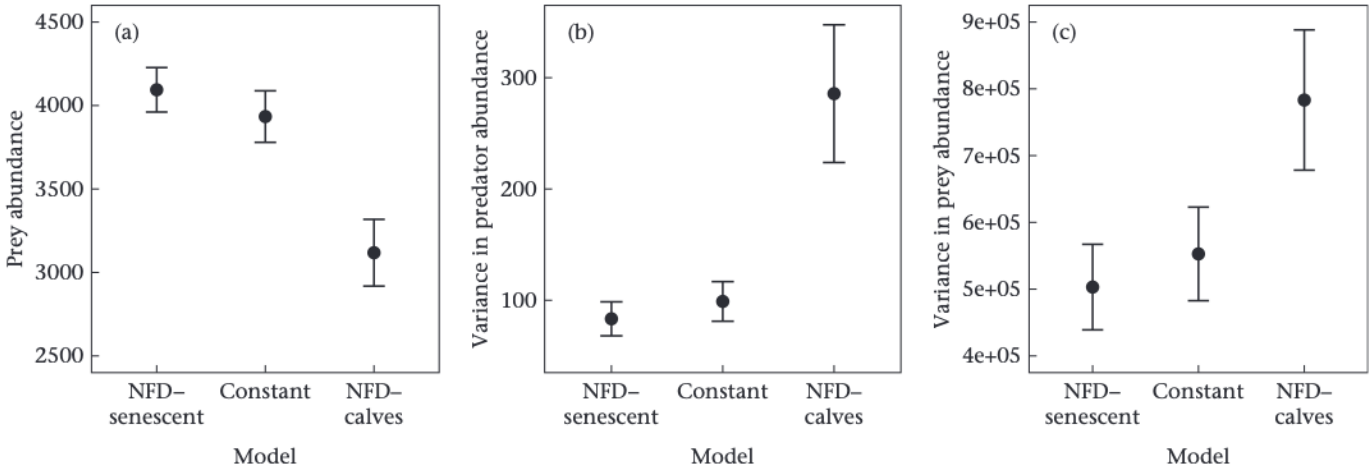

Figure 5. Results of simulations assessing the influence of negative frequency-dependent selective predation on (a) mean abundance of prey, (b) temporal variation in predator abundance and (c) variation in prey abundance. Other details are as described in the legend for Fig. 4.

would require an assessment of a wide range of circumstances, such as the degree to which different prey species prefer the same habitat (e.g. elk and bison in YNP; Tallian et al., 2017), the degree to which different sexes prefer different habitats (Ruckstuhl & Neuhaus, 2002) and the tendency for different age classes of a prey species to occupy different areas (Montgomery, Vucetich, Peterson, Roloff, & Millenbah, 2013).

Wolves' tendency to avoid prime-aged female elk more than prime-aged male elk is likely explained by the following circumstances. First, elk calves remain with their mothers during their first year of life and herds containing prime-age females are most likely to contain calves. And, when wolves attack a cow–calf pair, they tend to attack the calf first and stop attacking after the calf is killed. Second, predators are more likely to kill individuals in poor condition (Temple, 1987) and males tend to be in poorer body condition than females during the winter, due to the energetic costs of the autumn rut (Wilmers et al., 2020). The finding that wolves strongly avoid prime-aged females is also consistent with prior research suggesting that wolf predation is not a significant cause of mortality for prime-aged female elk outfitted with radiocollars (MacNulty et al., 2020).

Selection for calves may have become weaker as wolf abundance increased in both sites (Table 1, Fig. 3a). Insomuch as population size is often indicative of intraspecific competition, this pattern could be due to predators becoming less selective as competition increases in order to maintain kill rates. That interpretation is consistent with an experiment where predators (common shrew, *Sorex araneus*) reduced their selectivity for different-sized prey when competitors were present (Barnard & Brown, 1981). Moreover, the assumption that competition for food increases with predator abundance appears to be supported in both study systems insomuch as the ratio of prey per predator rapidly declined as wolf abundance increased (see Appendix 3, Fig. A10). Because wolf abundance is sometimes associated with mean pack size, it is plausible that the decline in selection for calves as wolf abundance increased (Table 1) may be tied to the prospect that larger packs are more successful at killing larger adult prey. However, this possibility is weakened by previous research, which found no effect of larger pack size (>4 wolves) on the success of wolves hunting adult elk, including adult males (MacNulty et al., 2012). Lastly, it is relevant to note that declines in selection for calves as wolf abundance increased were accompanied by an increase in selection for one or more adult age classes. In YNP, the decline in selectivity for calves as wolf abundance increased (Table 1) appeared to be offset by wolves exhibiting stronger selection for senescent male elk (Fig. 2a). For IRNP, the decline in selectivity for calves appeared to be offset by wolves exhibiting weaker avoidance for prime-aged moose as wolf abundance increased (see Appendix 3, Fig. A11).

Simulations

The simulations suggest that negative frequency-dependent selection for calves (like that observed in Isle Royale) resulted in substantively different predator–prey dynamics, as compared to the case where predators are selective for different stages, but that pattern of selection is constant over time. By contrast, negative frequency-dependent selection for senescent adults (like that observed in Yellowstone) resulted in fewer differences, as compared to the case where selection is constant over time (Fig. 5). This may be because both these models included strong, but constant, selection for calves. Below, we discuss the ecological relevance of the most striking differences that arose when selection for calves was negatively frequency dependent.

First, the per capita kill rate was less precisely predicted by the ratio of prey to predators (as indicated by lower slope and R^2 in Fig. 4a and i, respectively), due to two interacting circumstances. These circumstances were (1) per capita kill rate being a function of prey age structure (equations 1 and 2; Sand et al., 2012) and (2) the age structure of the prey population (frequency of calves and prime-aged individuals) exhibiting greater temporal variability when selection for calves was negatively frequency dependent (Appendix 3, Fig. A12). The greater significance of these results is that it leads to greater variance in the abundance of predators and their prey (see Fig. 5b and c).

Second, the predator was more efficient (sensu Roughgarden, 1979) in the sense that the slope of the numerical response was steeper (Fig. 4b). An important consequence of increased predator efficiency is that it tends to lower the predator isocline, resulting in a lower equilibrium for prey abundance (Gotelli, 2008). Indeed, mean prey abundance was ~20% lower when selection for calves was negatively frequency dependent (Fig. 5a). Lower prey abundance is also likely attributable to the higher mean predation rate (higher intercept in Fig. 4g).

Third, the slope of the relationship between predation rate and the per capita growth rate of the prey population was more strongly negative (Fig. 4d). That stronger negative slope is an indication that predation has a more destabilizing influence under those

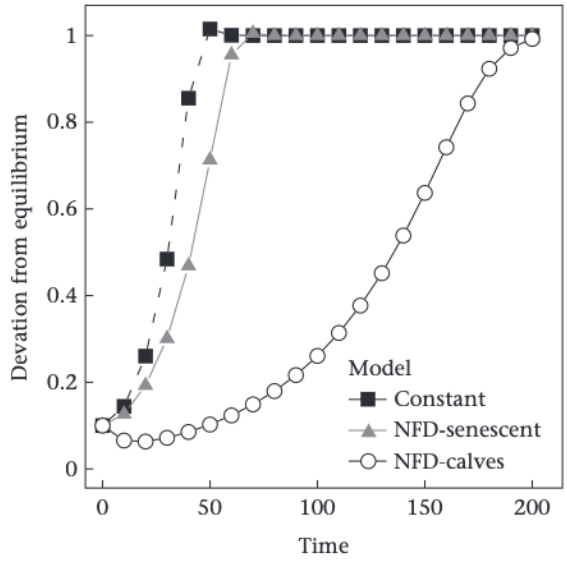

Figure 6. Results of simulations assessing the influence of negative frequency-dependent selective predation on return times to equilibrium following an exogenous perturbation (reduction to 10% of equilibrium) when environmental stochasticity is set to zero. The *Y* axis is scaled because the three models had different equilibrium values. Other details about the models being compared are as described in the legend for Fig. 4.

conditions. A manifestation of that destabilizing influence is indicated by the reduced resiliency (i.e. longer return times; Fig. 6). The stronger negative slope and lower resilience are most likely attributable to the increased predator efficiency and higher mean predation rate. Overall, the steeper negative slope of the relationship between predation rate and prey growth rate (Fig. 4d), the higher variability in predator and prey abundance (Fig. 5b and c) and the longer return times (following an exogenous perturbation; Fig. 6) are all consistent with predation being a more destabilizing force when selection for calves is negatively frequency dependent.

Although negative frequency-dependent selection for calves had destabilizing influences on population dynamics, negative frequency-dependent selection for senescent individuals did not result in those destabilizing influences. That difference is likely explained by two observations. First, negative frequency-dependent selection for calves was associated with increased temporal variability in the survival and relative abundance of calves (Appendix 3, Fig. A12), and the population dynamics of ungulates tend to be importantly driven by fluctuations in juvenile survival and recruitment (Gaillard, Festa-Bianchet, Yoccoz, Loison, & Toïgo, 2000). Second, ungulate reproduction is often negatively density dependent and senescent adults have less reproductive value than prime-aged adults. Consequently, any potentially destabilizing effect of negative frequency-dependent selection for senescent adults may be offset by the decline in survival for senescent adults reducing competition among the remaining prime-age individuals. Regardless of underlying mechanisms, the simulation results are valuable for revealing that negative frequency dependence had a significant destabilizing influence in some, but not all, cases.

To have observed destabilizing influences of negative frequency-dependent selection for calves and to observe that wolf–ungulate systems tend to persist does not represent an explanation-demanding paradox. Rather, a broad theme in population ecology is to understand the panoply of processes that tend to have stabilizing or destabilizing influences on a population. Destabilizing influences are often (not always) counterbalanced by stabilizing forces, such as density dependence, functional response dynamics and emigration/immigration.

In conclusion, Yellowstone and Isle Royale exhibited different patterns of dynamic selection, despite both study systems involving wolves who prey primarily on a large ungulate species. It is not yet clear how representative either pattern of negative frequency dependence is of other systems. Nevertheless, the observed selection dynamics resulted in important, although difficult to anticipate, effects on predator–prey dynamics. Additional worthwhile insights may be gained through future studies that assess the alternative mechanisms and the trade-offs associated with frequency-dependent selection for different age classes of prey.

Author Contributions

S.R.H. and J.A.V. conceived the ideas for the study, designed and carried out the analysis of empirical data and simulation analyses and led the writing of the manuscript. D.R.M., M.C.M., D.W.S., D.R.S. and R.O.P. contributed critically to data collection and reviewing and editing drafts.

Acknowledgments

We are grateful to the many volunteers, pilots and staff from the National Park Service and Montana Fish, Wildlife and Parks (MFWP) who helped collect elk and moose carcass data. This research was supported by funding from the U.S. National Science Foundation (DEB-0918247, DEB-0613730, DEB-1245373), Isle Royale National Park (CESU Task Agreement No. P11AC90808), Yellowstone National Park, the Robbins Chair in Sustainable Management of the Environment to R.O.P. at Michigan Technological University, McIntire-Stennis Grants USDA-NIFA-224870 and USDA-NIFA-1004363 (U.S. Department of Agriculture, National Institute of Food and Agriculture). Funding was also received from Yellowstone Park Foundation (now Yellowstone Forever) and many private donors, especially, Annie and Bob Graham, Valerie Gates and Frank and Kay Yeager.

References

Austin, P. C., & Steyerberg, E. W. (2015). The number of subjects per variable required in linear regression analyses. *Journal of Clinical Epidemiology, 68*(6), 627–636. https://doi.org/10.1016/j.jclinepi.2014.12.014

Barnard, C. J., & Brown, C. A. J. (1981). Prey size selection and competition in the common shrew (*Sorex araneus* L.). *Behavioral Ecology and Sociobiology, 8*, 239–243. https://doi.org/10.2307/4599387

Becker, M. S., Garrott, R. A., White, P. J., Jaffe, R., Borkowski, J. J., Gower, C. N., et al. (2009). Wolf kill rates: Predictably variable? In R. J. Garrott, P. J. White, & F. G. R. Watson (Eds.), *The ecology of large mammals in central Yellowstone: Sixteen years of integrated field studies* (pp. 339–369). Amsterdam, The Netherlands: Academic Press.

Berger-Tal, O., Mukherjee, S., Kotler, B. P., & Brown, J. S. (2009). Look before you leap: Is risk of injury a foraging cost? *Behavioral Ecology and Sociobiology, 63*(12), 1821–1827.

Boukal, D. S., Berec, L., & Křivan, V. (2008). Does sex-selective predation stabilize or destabilize predator–prey dynamics? *PLoS One, 3*(7), Article e2687.

Burnham, K. P., & Anderson, D. R. (2002). *Model selection and multimodel inference: A practical information-theoretic approach* (2nd ed.). New York, NY: Springer-Verlag.

Chan, K., Boutin, S., Hossie, T. J., Krebs, C. J., O'Donoghue, M., & Murray, D. L. (2017). Improving the assessment of predator functional responses by considering alternate prey and predator interactions. *Ecology, 98*(7), 1787–1796. https://doi.org/10.1002/ecy.1828

Chesson, J. (1978). Measuring preference in selective predation. *Ecology, 59*(2), 211–215. https://doi.org/10.2307/1936364

Chesson, J. (1983). The estimation and analysis of preference and its relationship to foraging models. *Ecology, 64*(5), 1297–1304. https://doi.org/10.2307/1937838

Edenius, L., Ericsson, G., & Näslund, P. (2002). Selectivity by moose vs the spatial distribution of aspen: A natural experiment. *Ecography, 25*, 289–294. https://doi.org/10.1034/j.1600-0587.2002.250305.x

Ellis, J. E., Wiens, J. A., Rodell, C. F., & Anway, J. C. (1976). A conceptual model of diet selection as an ecosystem process. *Journal of Theoretical Biology, 60*(1), 93–108. https://doi.org/10.1016/0022-5193(76)90157-0

Fryxell, J. M., Falls, J. B., Falls, E. A., Brooks, R. J., Dix, L., & Strickland, M. A. (1999). Density dependence, prey dependence, and population dynamics of martens in Ontario. *Ecology, 80*(4), 1311–1321.

Fuller, T. K., Mech, L. D., & Cochrane, J. F. (2003). Wolf population dynamics. In L. D. Mech & L. Boitani (Eds.), *Wolves: Behavior, ecology, and conservation* (pp. 161–191). Chicago, IL: Chicago University Press.

Gaillard, J.-M., Festa-Bianchet, M., Yoccoz, N. G., Loison, A., & Toïgo, C. (2000). Temporal variation in fitness components and population dynamics of large herbivores. *Annual Review of Ecology, Evolution, and Systematics, 31*, 367–393. https://doi.org/10.1146/annurev.ecolsys.31.1.367

Garrott, R. A., Bruggeman, J. E., Becker, M. S., Kalinowski, S. T., & White, P. J. (2007). Evaluating prey switching in wolf–ungulate systems. *Ecological Applications, 17*(6), 1588–1597.

Gervasi, V., Nilsen, E. B., Sand, H., Panzacchi, M., Rauset, G. R., Pedersen, H. C., et al. (2012). Predicting the potential demographic impact of predators on their prey: A comparative analysis of two carnivore–ungulate systems in Scandinavia. *Journal of Animal Ecology, 81*(2), 443–454.

Gotelli, N. J. (2008). *A primer of ecology* (4th ed.). Sunderland, MA: Sinauer.

Gove, N. E., Skalski, J. R., Zager, P., & Townsend, R. L. (2002). Statistical models for population reconstruction using age-at-harvest data. *Journal of Wildlife Management, 66*(2), 310–320. http://www.jstor.org/stable/3803163.

Haagenrud, H. (1978). Layers of secondary dentine in incisors as age criteria in moose. *Journal of Mammology, 59*, 857–858.

Hallet, T. B., Coulson, T., Pilkington, J. G., Clulton-Brock, T. H., Pemberion, J. M., & Grenfell, B. T. (2004). Why large-scale climate indices seem to predict ecological processes better than local weather. *Nature, 430*(6995), 71–75. https://doi.org/10.1038/nature02708

Hassell, M. P. (2000). *The spatial and temporal dynamics of host parasitoid interactions*. Oxford, U.K.: Oxford University Press.

Hassell, M. P., Lawton, J. H., & Beddington, J. R. (1976). The components of arthropod predation: I. The prey death-rate. *Journal of Animal Ecology, 45*(1), 135–164.

Houston, D. B. (1982). *The northern Yellowstone elk herd*. New York, NY: Macmillan.

Hoy, S. R., MacNulty, D. R., Smith, D. W., Stahler, D. R., Lambin, X., Peterson, R. O., et al. (2020). Fluctuations in age structure and their variable influence on population growth. *Functional Ecology, 34*(1), 203–216. https://doi.org/10.1111/1365-2435.13431

Hoy, S. R., Petty, S. J., Millon, A., Whitfield, D. P., Marquiss, M., Davison, M., et al. (2015). Age and sex-selective predation as moderators of the overall impact of predation. *Journal of Animal Ecology, 84*(3), 692–701.

Hoy, S. R., Vucetich, J. A., Liu, R., DeAngelis, D., Peterson, R. O., Vucetich, L. M., et al. (2019). Negative frequency-dependent foraging behaviour in a generalist herbivore (*Alces alces*) and its stabilizing influence on food web dynamics. *Journal of Animal Ecology, 88*(9), 1291–1304. https://doi.org/10.1111/1365-2656.13031

Hubbard, S. F., Cook, R. M., Glover, J. G., & Greenwood, J. J. D. (1982). Apostatic selection as an optimal foraging strategy. *Journal of Animal Ecology, 51*(2), 625–633. https://doi.org/10.2307/3987

Hughes, R. N., & Croy, M. I. (1993). An experimental analysis of frequency-dependent predation (switching) in the 15-spined stickleback, *Spinachia spinachia*. *Journal of Animal Ecology, 62*(2), 341–352. https://doi.org/10.2307/5365

Hurrell, J. (1995). *Hurrell North Atlantic Oscillation (NAO) Index 390 (station-based)*. https://climatedataguide.ucar.edu/climate-data/hurrell-north-atlantic-oscillation-nao-index-station-based.

MacArthur, R. H., & Pianka, E. R. (1966). On optimal use of a patchy environment. *American Naturalist, 100*(916), 603–609. https://doi.org/10.1086/282454

MacNulty, D. R., Smith, D. W., Mech, L. D., Vucetich, J. A., & Packer, C. (2012). Nonlinear effects of group size on the success of wolves hunting elk. *Behavioral Ecology, 23*(1), 75–82. https://doi.org/10.1093/beheco/arr159

MacNulty, D. R., Stahler, D. R., Wyman, T., Ruprecht, J., Smith, L. M., Kohl, M. T., et al. (2020). Population dynamics of northern Yellowstone elk after wolf reintroduction. In D. W. Smith, D. R. Stahler, & D. R. MacNulty (Eds.), *Yellowstone wolves: Science and discovery in the world's first national park* (pp. 184–199). Chicago, IL: University of Chicago Press. https://press.uchicago.edu/ucp/books/book/chicago/Y/bo60080807.html.

Magnhagen, C. (1991). Predation risk as a cost of reproduction. *Trends in Ecology & Evolution, 6*(6), 183–186. https://doi.org/10.1016/0169-5347(91)90210-O

Manly, B. F. J. (1974). A model for certain types of selection experiments. *Biometrics, 30*(2), 281–294. https://doi.org/10.2307/2529649

Mech, L. D., McRoberts, R. E., Peterson, R. O., & Page, R. E. (1987). Relationship of deer and moose populations to previous winters' snow. *Journal of Animal Ecology, 56*(2), 615–627. https://doi.org/10.2307/5072

Metz, M. C., Smith, D. W., Vucetich, J. A., Stahler, D. R., & Peterson, R. O. (2012). Seasonal patterns of predation for gray wolves in the multi-prey system of Yellowstone National Park. *Journal of Animal Ecology, 81*(3), 553–563. https://doi.org/10.1111/J.1365-2656.2011.01945.X

Montgomery, R. A., Vucetich, J. A., Peterson, R. O., Roloff, G. J., & Millenbah, K. F. (2013). The influence of winter severity, predation and senescence on moose habitat use. *Journal of Animal Ecology, 82*(2), 301–309. https://doi.org/10.1111/1365-2656.12000

Montgomery, R. A., Vucetich, J. A., Roloff, G. J., Bump, J. K., & Peterson, R. O. (2014). Where wolves kill moose: The influence of prey life history dynamics on the landscape ecology of predation. *PLoS One, 9*(3), Article e91414. https://doi.org/10.1371/journal.pone.0091414

Mukherjee, S., & Heithaus, M. R. (2013). Dangerous prey and daring predators: A review. *Biological Reviews, 88*(3), 550–563. https://doi.org/10.1111/brv.12014

Murdoch, W. W. (1969). Switching in general predators: Experiments on predator specificity and stability of prey populations. *Ecological Monographs, 39*(4), 335–354. https://doi.org/10.2307/1942352

Murdoch, W. W., & Oaten, A. (1975). Predation and population stability. *Advances in Ecological Research, 9*, 1–131. https://doi.org/10.1016/S0065-2504(08)60288-3

Nussey, D. H., Froy, H., Lemaitre, J. F., Gaillard, J. M., & Austad, S. N. (2013). Senescence in natural populations of animals: Widespread evidence and its implications for bio-gerontology. *Ageing Research Reviews, 12*(1), 214–225.

Oaten, A., & Murdoch, W. W. (1975). Switching, functional response, and stability in predator–prey systems. *American Naturalist, 109*(967), 299–318. https://doi.org/10.1086/282999

O'Donoghue, M., Boutin, S., Krebs, C. J., Zuleta, G., Murray, D. L., & Hofer, E. J. (1998). Functional responses of coyotes and lynx to the snowshoe hare cycle. *Ecology, 79*(4), 1193–1208. https://doi.org/10.1890/0012-9658(1998)079[1193:FROCAL]2.0.CO;2

Parker, K. L., Robbins, C. T., & Hanley, T. A. (1984). Energy expenditures for locomotion by mule deer and elk. *Journal of Wildlife Management, 48*(2), 474–488. https://doi.org/10.2307/3801180

Peterson, R. O. (1977). Wolf ecology and prey relationships on Isle Royale *[Scientific Monograph Series 11]*. Washington, D.C.: U.S. Department of the Interior, U.S. National Park Service.

Peterson, R. O., & Page, R. E. (1988). The rise and fall of Isle Royale wolves, 1975–1986. *Journal of Mammalogy, 69*(1), 89–99. https://doi.org/10.2307/1381751

Peterson, R. O., Thomas, N. J., Thurber, J. M., Vucetich, J. A., & Waite, T. A. (1998). Population limitation and the wolves of Isle Royale. *Journal of Mammalogy, 79*(3), 828–841. https://doi.org/10.2307/1383091

Peterson, R. O., Vucetich, J. A., Bump, J. M., & Smith, D. W. (2014). Trophic cascades in a multicausal world: Isle Royale and Yellowstone. *Annual Review Ecology Evolution and Systematics, 45*, 325–345.

Pimm, S. L. (1991). *The balance of nature? Ecological issues in the conservation of species and communities*. Chicago, IL: University of Chicago Press.

Post, E., Peterson, R. O., Stenseth, N. C., & McLaren, B. E. (1999). Ecosystem consequences of wolf behavioural response to climate. *Nature, 401*(6756), 905–907.

R Core Development Team. (2015). *R: A language and environment for statistical computing*. Vienna, Austria: R Foundation for Statistical Computing. https://www.r-project.org/.

Reimer, J. R., Brown, H., Beltaos-Kerr, E., & de Vries, G. (2019). Evidence of intraspecific prey switching: Stage-structured predation of polar bears on ringed seals. *Oecologia, 189*(1), 133–148. https://doi.org/10.1007/s00442-018-4297-x

Rolandsen, C. M., Solberg, E. J., Heim, M., Holmstrøm, F., Solem, M. I., & Sæther, B. E. (2008). Accuracy and repeatability of moose (*Alces alces*) age as estimated from dental cement layers. *European Journal of Wildlife Research, 54*(1), 6–14. https://doi.org/10.1007/s10344-007-0100-8

Roughgarden, J. (1979). *Theory of population genetics and evolutionary ecology: An introduction*. New York, NY: Macmillan.

Ruckstuhl, K. E., & Neuhaus, P. (2002). Sexual segregation in ungulates: A comparative test of three hypotheses. *Biological Reviews of the Cambridge Philosophical Society, 77*(1), 77–96. https://doi.org/10.1017/S1464793101005814

Sand, H., Vucetich, J. A., Zimmermann, B., Wabakken, P., Wikenros, C., Pedersen, H. C., et al. (2012). Assessing the influence of prey–predator ratio, prey age structure and packs size on wolf kill rates. *Oikos, 129*, 1454–1463.

Smith, D. W., & Bangs, E. E. (2009). Reintroduction of wolves to Yellowstone national park: History, values and ecosystem restoration. In M. W. Hayward, & M. Sommers (Eds.), *Reintroduction of top-order predators* (pp. 92–125). Chichester, U.K: Wiley-Blackwell. https://doi.org/10.1002/9781444312034.ch5.

Solberg, E. J., Sæther, B.-E., Strand, O., & Loison, A. (1999). Dynamics of a harvested moose population in a variable environment. *Journal of Animal Ecology, 68*(1), 186–204.

Stelfox, J. G. (1971). Bighorn sheep in the Canadian rockies: A history 1800–1970. *Canadian Field-Naturalist, 85*, 101–122.

Stephens, D. W., & Krebs, J. R. (1986). *Foraging theory*. Princeton, NJ: Princeton University Press.

Tallian, A., Smith, D. W., Stahler, D. R., Metz, M., Wallen, R., Geremia, C., et al. (2017). Predator foraging response to a resurgent dangerous prey. *Functional Ecology, 31*(7), 1418–1429.

Temple, S. A. (1987). Do predators always capture substandard individuals disproportionately from prey populations? *Ecology, 68*(3), 669–674.

Uhazy, L. S., Holmes, J. C., & Stelfox, J. G. (1973). Lungworms in the Rocky Mountain bighorn sheep of western Canada. *Canadian Journal of Zoology, 51*, 817–824. https://doi.org/10.1139/z73-122

Vittinghoff, E., & McCulloch, C. E. (2007). Relaxing the rule of ten events per variable in logistic and Cox regression. *American Journal of Epidemiology, 165*(6), 710–718.

Vucetich, J. A., Hebblewhite, M., Smith, D. W., & Peterson, R. O. (2011). Predicting prey population dynamics from kill rate, predation rate and predator–prey ratios in three wolf–ungulate systems. *Journal of Animal Ecology, 80*(6), 1236–1245. https://doi.org/10.1111/j.1365-2656.2011.01855.x

Vucetich, J. A., & Peterson, R. O. (2004). The influence of top–down, bottom–up and abiotic factors on the moose (*Alces alces*) population of Isle Royale. *Proceedings of the Royal Society: Biological Science, 271*(1535), 183–189.

Vucetich, J. A., Peterson, R. O., & Schaefer, C. L. (2002). The effect of prey and predator densities on wolf predation. *Ecology, 83*(11), 3003–3013. https://doi.org/10.1890/0012-9658(2002)083[3003:TEOPAP]2.0.CO;2

Werner, E. E., & Hall, D. J. (1974). Optimal foraging and the size selection of prey by the bluegill sunfish (*Lepomis macrochirus*). *Ecology, 55*(5), 1042–1052. https://doi.org/10.2307/1940354

Wilmers, C. C., Metz, M. C., Stahler, D. R., Kohl, M. T., Geremia, C., & Smith, D. W. (2020). How climate impacts the composition of wolf-killed elk in northern Yellowstone National Park. *Journal of Animal Ecology, 89*(6), 1511–1519. https://doi.org/10.1111/1365-2656.13200

Wockner, G., Singer, F., Coughenour, M., & Farnes, P. (2002). *Application of a snow model for Yellowstone National Park*. Ft Collins, CO: Natural Resources Ecology Lab, Colorado State University. https://mountainscholar.org/handle/10217/231604.

Wright, G. J., Peterson, R. O., Smith, D. W., & Lemke, T. O. (2006). Selection of northern Yellowstone elk by gray wolves and hunters. *Journal of Wildlife Management, 70*, 1070–1078.

Young, T. (1994). Natural die-offs of large mammals: Implications for conservation. *Conservation Biology, 8*(2), 410–418. https://www.jstor.org/stable/2386465?seq=1.

Appendix 1

Age-specific Ungulate Survival and Assessing Frequency-dependent Selection by Wolves for Demographic Classes of Elk and Moose

Assessing frequency-dependent selection

To assess the impact of selective foraging behaviour on predator–prey dynamics (Figs 4, 5), it is essential to first understand the relationship between the environmental frequency (e_i) of a food type and selection (α_i) because α modifies the attack rate in the functional response of consumer resource models (see equation 2 in main text). However, statistical assessments of the relationship between e_i and α_i merit special care because e_i and α_i have a built-in statistical dependency (see equation 1 in main text). There is a potential concern that these statistical dependencies could lead to biased inferences about the slope of the e_i and α_i relationship and misleading conclusions about whether selection is negatively frequency dependent (as indicated in Figs 2 and 3 in the main text). That concern can be allayed by recognizing that (1) the relationship between e_i and α_i directly corresponds to a specific relationship between e_i and dietary frequency (r_i) as illustrated in Fig. A3 and (2) statistical assessments of the observed relationship between e_i and r_i are not complicated by built-in statistical dependencies because r_i can be calculated independently of e_i.

Below we demonstrate that inferences about negative frequency-dependent selection based on the relationship between e_i and α_i (Figs 2 and 3 in main text) are also supported by inferences made from empirical assessments of the relationships between e_i and r_i.

Selection for senescent male elk

First, we re-evaluate the e_i and α_i relationship for senescent male elk (Fig. 2a). That relationship is depicted in Fig. A4a when m is set to 2, which represents wolf diets consisting of two food types: senescent males and all other kinds of elk. (Note the values for α_i in Fig. A4 where $m = 2$ will differ from those in Fig. 2a where $m = 5$). The red line in Fig. A4a represents a null hypothesis for wolves showing strong selection for senescent male elk, but selection is independent of environmental frequency (see Table A1 for details). The red line in Fig. A4b represents the same null hypothesis expressed in terms of e_i and r_i (calculated using the equation in Fig. A3). The black line in Fig. A4a is the linear model that best fits the observed data. For emphasis, the observed data [e_i, r_i] in Fig. A4b are estimated independently (see main text). The black line in Fig. A4a has an estimated slope of -3.54 (± SE 0.74, $P = 0.001$), which represents prima facie evidence for negative frequency dependence. The appropriateness of that conclusion is also supported by the e_i and r_i relationship in Fig. A4b. In particular, when selection is negatively frequency dependent, the e_i and r_i relationship is expected to have an intercept that is significantly higher and a slope significantly lower than the null case, where selection is independent of frequency (see Fig. A3). Fig. A4b suggests the best-fitting model for the observed data (grey line) has a slope and intercept that are significantly different from the red line predicted by the null hypothesis (slope: $P = 0.003$ (left-tailed t test), intercept: $P - 0.002$ (right-tailed t test)).

For clarity, note that those P values correspond to a test for whether the intercept and slope of the grey line were significantly different from a linear approximation of the red line. In that regard, it is important to know that 99% of the variance in the red line is explained by a linear model. Also note, the similarity between the black and grey lines in panel Fig. A4b provides further reassurance that selection is negatively frequency dependent because the black line in panel Fig. A4b directly corresponds to the black line in Fig. A4a (calculated using the equation in Fig. A3).

Selection for senescent female elk

We used the same approach described above to assess selection for senescent female elk (Fig. 2b). The black line in Fig. A5a is the best-fitting linear model to the observed relationship between e_i and α_i for senescent females when $m = 2$. That black line has an estimated slope -1.46 (± 0.15 SE; $P < 10^{-5}$), which also represents evidence for negative frequency dependence. That conclusion is further supported by the relationship between e_i and r_i depicted in Fig. A5b. Specifically, the best-fitting model for the observed data in Fig. A5b (grey line) has a slope that is significantly lower and an intercept that is significantly higher than the red line predicted by the null model (slope: $P < 10^{-5}$ (left-tailed t test); intercept: $P < 10^{-4}$ (right-tailed t test)).

Note, the black line in Fig. A5b is calculated from the black line in Fig. A5a and is provided only for reference. It is not surprising or problematic that the black line in Fig. A5b is nonlinear because the grey line upon which our test of the null hypothesis is based is linear.

Selection for moose calves

Next we use the same approach described above to assess selection for moose calves (Fig. 3a) in IRNP when $m = 2$ (see Fig. A6 below). The black line in Fig. A6a is the best-fitting model for the observed relationship between e_i and α_i for moose calves. That black line has an estimated slope of -1.88 (± SE 0.53; $P - 0.001$), which suggests selection is negatively frequency dependent. The relationship between e_i and r_i depicted in Fig. A6b is also consistent with selection for calves being negatively frequency dependent. More precisely, the best-fitting model for the observed data (grey line) has a slope that is significantly lower and an intercept that is significantly higher than the red line predicted by the null model (slope: $P = 0.003$ (left-tailed t test); intercept: $P = 0.001$ (right-tailed t test)).

Selection for senescent moose

Lastly, we use the same approach to assess selection for senescent moose in IRNP (Fig. 3b). The black line in Fig. A7a is the best-fitting model for the observed relationship between e_i and α_i for senescent moose and has an estimated slope of -0.53 (± SE 0.19; $P = 0.007$). The best-fitting model for the observed relationship between e_i and r_i (grey line in Fig. A7b) has a slope that is significantly lower and an intercept that is significantly higher than the red line predicted by the null model (slope: $P = 0.001$ (left-tailed); intercept: $P - 0.001$ (right-tailed)). Both of these results are consistent with selection for senescent moose being negatively frequency dependent.

Note that, although the red and black lines in Fig. A7b are nonlinear, they are well approximated by a linear model. Specifically, 99% of the variance in the red line and 95% of the variance in the black line are explained by linear models.

Summary

The preceding account demonstrates that inferences about negative frequency dependence as represented by Figs 2 and 3

of the main text are also supported by analyses of the e_i and r_i relationship. Therefore, the statistical dependencies between e_i and α_i do not appear to result in biased inferences about whether selection is negatively frequency dependent. The results of this preceding account are also summarized in the Table A1 below.

Appendix 2

Predator–Prey Model Used to Assess the Community Level Consequences of Predators Exhibiting Selective Foraging Dynamics

Prey population model

The prey population was characterized by a single sex model with three life-history stages (calves, prime-aged, senescent) for a generic large ungulate species. Specifically, the calf stage cannot reproduce, the survival and fecundity of prime-aged adults is higher than for senescent adults and individuals can remain in the prime-age class for a number of years before becoming senescent. The equations for stage-specific prey demography are:

$$N_{t+1,1} = f_t(\cdot)N_{t,2} + g_t(\cdot)N_{t,3} - P_t x_{t,1} \quad \text{(A1)}$$

$$N_{t+1,2} = a_{2,1}N_{t,1} + a_{2,2}N_{t,2} - P_t x_{t,2} \quad \text{(A2)}$$

$$N_{t+1,3} = a_{3,2}N_{t,2} + a_{3,3}N_{t,3} \quad P_t x_{t,3}, \quad \text{(A3)}$$

where $N_{t,i}$ is the number of prey in each life-history stage i (i.e. calf, prime-aged, senescent) at time t, P_t is predator abundance, a values are transition probabilities and $f(\cdot)$ and g $(\cdot)$ are stochastic, density-dependent terms. In particular, we used a nonlinear equation to model density dependence (Varley & Boyce, 2006):

$$f_t = \frac{1}{Q + \exp[V + YN_{t-1,\,\text{total}}]} + \varepsilon_t, \quad \text{(A4)}$$

where Q, V and Y determine the shape of density-dependence and ε_t represents environmental stochasticity. We set $Q = 2.9$, $V = -6.5$ and $Y = 1.43 \times 10^{-3}$, which results in a density-dependent fecundity function that is representative of a large ungulate (Fig. A8). We set $g_t(\cdot) = f_t(\cdot) \times 0.8$ such that the fecundity of senescent adults was 20% lower than fecundity for prime-aged adults for any given density. We modelled environmental stochasticity as an autocorrelated and bounded, random walk:

$$\varepsilon_t = \varepsilon_{t-1} + \gamma_t, \quad \text{if } 0.09 > \varepsilon_t > -0.09, \quad \text{(A5)}$$

$$\text{if } \varepsilon_t > 0.09, \text{ then } \varepsilon_t \text{ was reset to } 0.09 - (\varepsilon_t - 0.09), \quad \text{(A6)}$$

$$\text{if } \varepsilon_t < 0.09, \text{ the } \varepsilon_t \text{ was reset to } 0.09 + (0.09 - \varepsilon_t), \quad \text{(A7)}$$

where γ_t is a NID $(0,\sigma^2)$ random variable and $\sigma = 0.02$. Equations (A6) and (A7) represent a reflecting boundary, whereby the reset value of ε_t is as far inside the boundary as it had been originally set to be outside the boundary. The magnitude of the upper and lower boundaries in equation (A5) represent 30% of 0.3, which represents the expected mean probability of producing a female calf. Autocorrelation is necessary to drive fluctuations in age structure like those observed in moose in IRNP and elk in YNP (Hoy et al., 2020). If equation (A5) caused f_t to exceed 0.4 or be lower than 0.15, then we reset f_t for that time step to be 0.4 or 0.15, respectively.

In equation (A2), the two transition probabilities are $a_{2,1} = 0.65$, which is the probability that calves are recruited into the population of adults, and

$$a_{2,2} = \left(\frac{1 - s^{d-1}}{1 - s^d}\right)s, \quad \text{(A8)}$$

where $s = 0.95$ is the annual survival rate of prime-aged adults and $d = 8$ is the number of years that individuals can remain in the prime-age stage class (i.e. 1–8 years of age).

For equation (A3), the two transition probabilities are $a_{3,3} = 0.7$, which is the probability of survival for senescent individuals, and

$$a_{3,2} = \frac{s^d(1 - s)}{1 - s^d}, \quad \text{(A9)}$$

which is the probability of a prime-aged individual transitioning to the senescent stage. We set $a_{2,1}$, s, $a_{3,3}$ and $a_{3,2}$ to values that are characteristic of large ungulates and yield a stable stage distribution similar to that observed in IRNP and YNP (i.e. approximately 15% calves, 65% prime-aged and 20% senescent adults).

Predator population model

For the predator model, we used a type II ratio-dependent functional response, modified to account for α (Chan et al., 2017):

$$x_{i,t} = (\alpha_{i,t}zN_{i,t})/(P_t + \alpha_{i,t}zh_iN_{i,t}), \quad \text{(A10)}$$

here z is the attack rate, h_i is the handling time and i is an index for prey stage. Ratio dependency is justified by empirical assessments of both study populations (Becker et al., 2009; Vucetich et al., 2002). The predator equation (Hassell et al., 1976; Vucetich & Peterson, 2004) is:

$$P_{t+1} = P_t(b_0 + b_1X_t), \quad \text{(A11)}$$

where b_0 and b_1 are the intercept and slope of the predator's numerical response. We used the parameter values: $b_0 = -0.302$, $b_1 = 0.072$. These values approximate those found in a thoroughly studied example in the published literature that examined the relationship between per capita kill rate and growth rate in a wolf population (i.e. Vucetich & Peterson, 2004). These values have also previously been used as default parameter values in prior simulations using predator–prey models (Hoy et al., 2019). X_t is the total number of prey killed per predator per unit of time, adjusted to account for the smaller body size of calves, which is equal to:

$$X_t = 0.38x_{1,t} + x_{2,t} + x_{3,t} \quad \text{(A12)}$$

The value 0.38 is equal to 114/((330 + 261)/2), where 114, 261 and 361 are mean weights (kg) of the edible portion of the carcasses of moose calves, adult females and adult males, respectively (Vucetich et al., 2004). For the same reason, we set h_1 equal to $0.38 \times h_2$ and $h_2 = h_3$. We set $z = 0.1$ and $h_2 = h_3 = 0.57$ to result in ungulate-to-wolf ratios ranging between 50 and 100, which is within range of ratios commonly observed (Fuller et al., 2003). We used initial population sizes of 3500 prey and 50 predators, which yields a starting prey–predator ratio of 70.

Predator selection dynamics

We built three versions of the predator–prey model, which were identical except for the pattern of frequency-dependent selection exhibited by the predator. For the first model (referred to as the constant model in figure captions), we set α_i to constant values ($\alpha_1 = 0.53$, $\alpha_2 = 0.08$, $\alpha_3 = 0.39$). These values are the

long-term average values for IRNP and are similar to long-term average values for YNP ($\alpha_1 = 0.58$, $\alpha_2 = 0.04$, $\alpha_3 = 0.39$).

For the second model (NFD-senescent model), we used linear functions to approximate the frequency-dependent pattern of selective predation by wolves observed in YNP, with selection for senescent adults declining as senescent adults become more common in the prey population (Fig. A9a):

$$\alpha_1 = 0.5, \tag{A13}$$

$$\alpha_2 = 1 - \alpha_1 - \alpha_3, \tag{A14}$$

$$\alpha_3 = 0.504 - 0.462[N_3 / N_{\text{total}}]. \tag{A15}$$

The value $\alpha_1 = 0.5$ reflects YNP wolves' strong selection for calves, independent of the environmental frequency of calves' in the population. We set $\alpha_2 = 1 - \alpha_1 - \alpha_3$, so that the sum of α values = 1.

For the third model (NFD-calves model), we used linear functions to approximate the frequency-dependent pattern of selective predation by wolves observed in IRNP, with selection for calves declining strongly as calves become more common (Fig. A9b) and selection for senescent adults to decline weakly as senescent adults become more common (Fig. A9c):

$$\alpha_1 = 0.925 - 3.067[N_1 / N_{\text{total}}], \tag{A16}$$

$$\alpha_2 = 1 - \alpha_1 - \alpha_3, \tag{A17}$$

$$\alpha_3 = 0.527 - 0.666[N_3 / N_{\text{total}}]. \tag{A18}$$

Note that for all the three versions of the model, we did not include an error term (to introduce stochasticity) into the functions determining the relationship between α_i and environmental frequency because the models already included a source of stochasticity. Introducing stochasticity (i.e. adding an error term) into the function determining the relationship between α_i and environmental frequency would also make it difficult to determine the impact(s) that changing the slope of this relationship has on predator–prey dynamics – which is the primary objective of these simulations.

Simulations and sensitivity analysis

For each of the three models (constant, NFD-senescent, NFD-calves), we simulated prey and predator population dynamics over a 200-year period and then discarded the first 50 years as burn-in. First, we ran simulations where all parameter values were set to the aforementioned default values. We also performed sensitivity analysis by adjusting a subset of five parameters that determine kill rates (attack rate, z in equation A10, the growth of the predator population (intercept and slope of numerical response, b_0 and b_1 in equation A11) and the growth of the prey population (the shape and strength of density-dependent recruitment by adjusting parameters V and Y in equation A4; see also Fig. A8). More precisely, each of the five parameters was varied, one at a time, by plus and minus 20% of the baseline level. This approach for conducting sensitivity analysis is similar to Hoy et al. (2019). Each combination of parameter settings was run for 10 replicates, yielding a total of 110 replicate simulations: one set of 10 replicates with all parameters set baseline values, five sets of 10 replicates where one of the five parameters is adjusted downward and five sets of 10 replicates where one of the five parameters is adjusted upward. The results of the sensitivity analysis are presented in Figs 4 and 5 in the main text.

Appendix 3

Additional Results Referred to in the Discussion of the Main Text

In the main text we make the inference that our results (Figs 2, 3) are not consistent with the prey-switching hypothesis. Here we provide some additional support for that inference. More precisely, if predators were exhibiting prey-switching behaviour, then one would expect predation on alternative prey types (i.e. prime-aged adults) to increase in years when the primary prey type (i.e. calves or senescent adults) were relatively rare. Therefore, we used linear models to assess whether the relative frequency of prime-aged moose or elk in wolf diets (hereafter, dietary frequency) was related to the relative frequency of either calves or senescent adults in the prey populations (hereafter environmental frequency). We considered whether those relationships were best characterized by a linear, log-transformed, exponential-transformed or second-order polynomial because prey-switching can result in nonlinear relationships.

Those analysis revealed that predation on alternative prey (prime-aged adults) did not increase in years when preferred prey were relatively rare in either study site. More precisely, dietary frequency of prime-aged male elk was not related to the environmental frequency of calves ($P > 0.31$) or senescent male elk ($P > 0.65$) in YNP. The dietary frequency of prime-aged female elk was also not related to either the environmental frequency of calves ($P > 0.76$) or senescent female elk ($P > 0.30$). In IRNP, there was no evidence to suggest that the dietary frequency of prime-aged moose was related to either the environmental frequency of calves ($P > 0.07$) or senescent adults ($P > 0.07$). Therefore, these results are not consistent with wolves exhibiting prey-switching behaviour.

Table A1
Summary of the intercepts (β_0) and slopes (β_1) associated with the relationships depicted in Figs A4-A7 above

Prey type	Observed e_i–α relationship (Coefficient ± SE)	Observed e_i–r_i relationship (Coefficient ± SE)	Null hypothesis e_i–α relationship	Null hypothesis e_i–r_i relationship	Test of the null hypothesis (P value)
Senescent male elk (Fig. 2a)	$\beta_0 = 1.09 \pm 0.08$	$\beta_0 = 0.38 \pm 0.09$	$\beta_0 = 0.71$	$\beta_0 = 0.04$	β_0: $P = 0.002$
	$\beta_1 = -3.54 \pm 0.74$	$\beta_1 = -1.21 \pm 0.84$	$\beta_1 = 0$	$\beta_1 = 1.74$	β_1: $P = 0.003$
Senescent female elk (Fig. 2b)	$\beta_0 = 0.91 \pm 0.03$	$\beta_0 = 0.24 \pm 0.03$	$\beta_0 = 0.70$	$\beta_0 = 0.04$	β_0: $P < 10^{-4}$
	$\beta_1 = -1.46 \pm 0.15$	$\beta_1 = 0.21 \pm 0.18$	$\beta_1 = 0$	$\beta_1 = 1.60$	β_1: $P < 10^{-5}$
Moose calves (Fig. 3a)	$\beta_0 = 0.995 \pm 0.07$	$\beta_0 = 0.34 \pm 0.08$	$\beta_0 = 0.75$	$\beta_0 = 0.06$	β_0: $P = 0.001$
	$\beta_1 = -1.88 \pm 0.53$	$\beta_1 = 0.05 \pm 0.63$	$\beta_1 = 0$	$\beta_1 = 1.86$	β_1: $P = 0.003$
Senescent moose (Fig. 3b)	$\beta_0 = 0.79 \pm 0.04$	$\beta_0 = 0.25 \pm 0.05$	$\beta_0 = 0.68$	$\beta_0 = 0.08$	β_0: $P = 0.001$
	$\beta_1 = -0.53 \pm 0.19$	$\beta_1 = 0.61 \pm 0.20$	$\beta_1 = 0$	$\beta_1 = 1.25$	β_1: $P = 0.001$

The second column contains coefficients for the black line in panel (a) of Figs A4-A7. The third column contains coefficients for the grey lines. The fourth column contains coefficients for red lines in panel (b) of Figs A4-A7, which represent the null hypothesis that wolves are exhibiting selection for each age class of prey, but selection is independent of environmental frequency. More precisely, the e_i–α relationship associated with the null hypothesis (fourth column) has an intercept that is equal to the mean level of selection (α) observed over the study period for each prey type and a slope = 0. The fifth column contains coefficients for a linear model approximating the red lines in panel (b) of Figs A4-A7 which represents the null hypothesis expressed in terms of the e_i–r_i relationship. The final column contains P values associated with a t test of whether the observed relationship between e_i and r_i (see third column and grey lines in panels (b) of Figs A4-A7) have a slope that is significantly lower (left-tailed), and an intercept that is significantly higher (right tailed) than the expected e_i and r_i relationship predicted by the null model (see fifth column and red lines in panels (b) of Figs A4-A7).

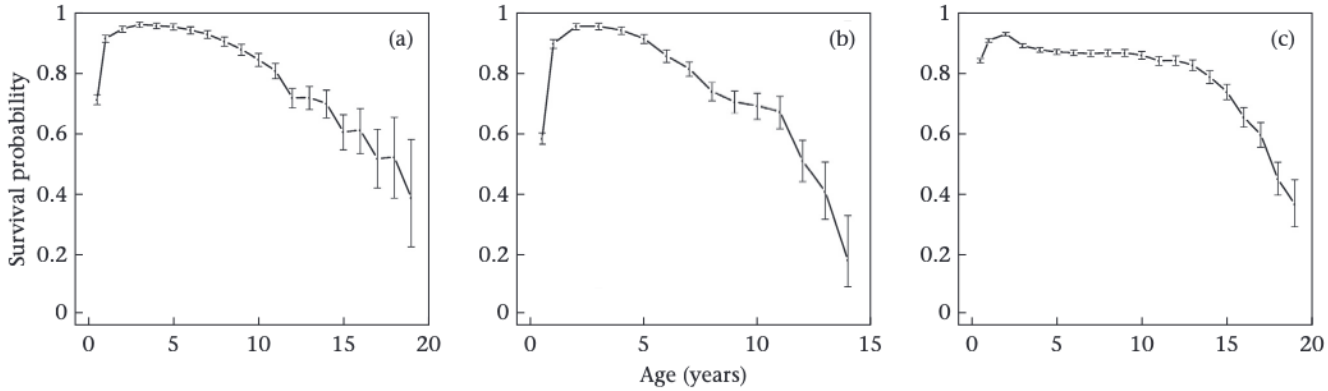

Figure A1. Age-specific survival rate (± 95% confidence interval) for (a) moose in Isle Royale National Park and (b) male elk and (c) female elk wintering along the northern border of Yellowstone National Park, as estimated from a known-fate-survival analysis based on dead recovery data. For details on data collection and methods see Hoy et al. (2020). Survival starts to decline much more rapidly with age for moose over 10 years old, male elk over 6 years old and female elk over 13 years.

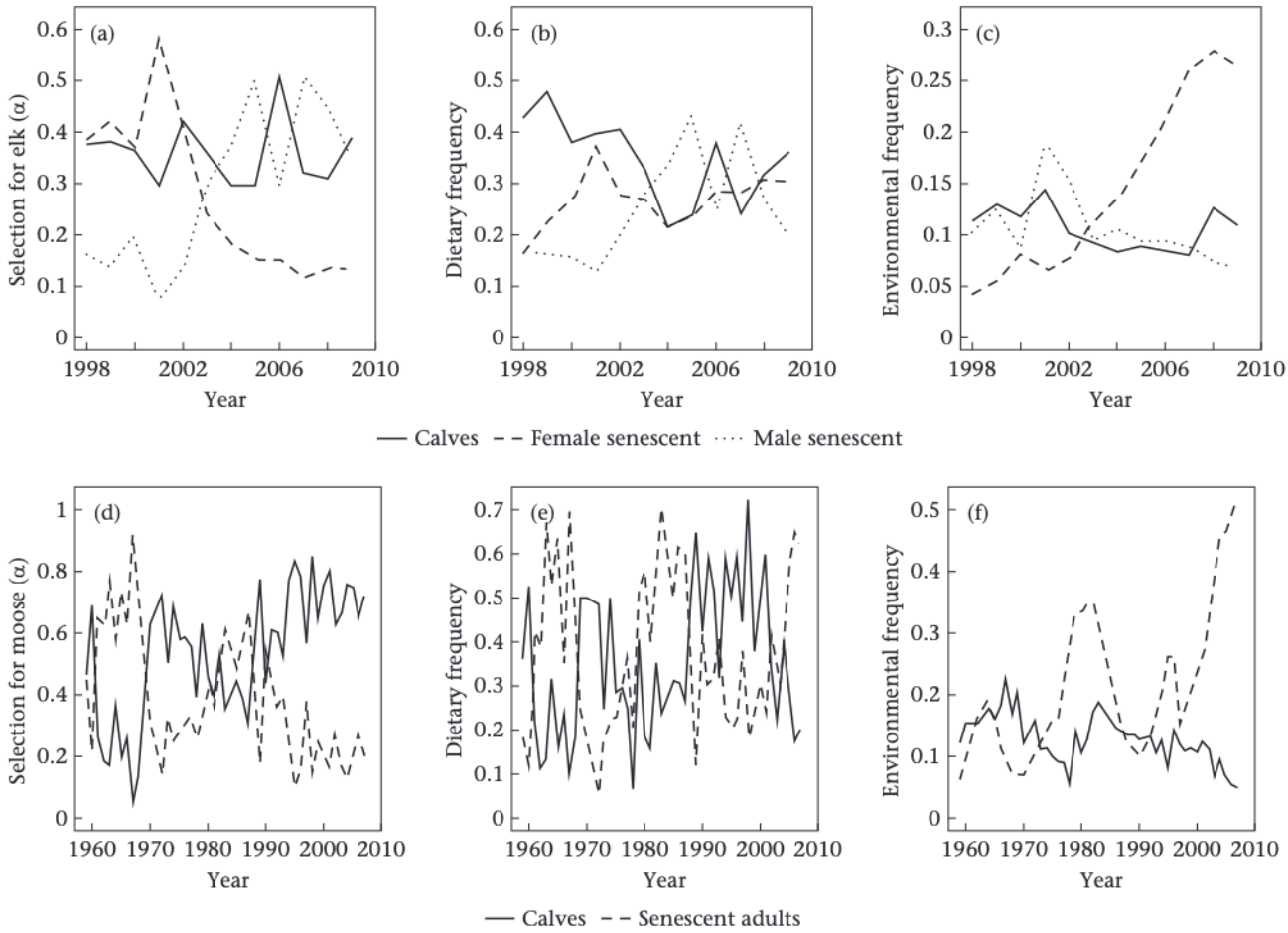

Figure A2. Temporal variation in (a) selection for different demographic classes of elk by wolves in Yellowstone National Park, (b) the frequency of demographic classes of elk in Yellowstone wolf diets, (c) the frequency of demographic classes in the Yellowstone elk population, (d) selection for different demographic classes of moose by wolves in Isle Royale National Park, (e) the frequency of demographic classes of moose in Isle Royale wolf diets and (f) the frequency of demographic classes in the Isle Royale moose population.

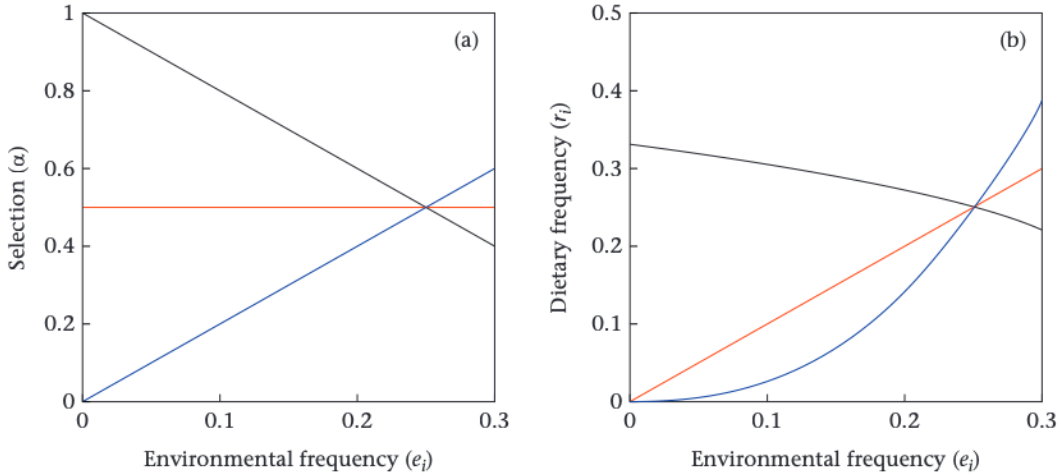

Figure A3. Lines of the same colour correspond to the same relationship expressed in different terms: (a) e_i versus α_i and (b) e_i versus r_i. The mapping from one panel to the other is possible because equation (1) in the main text can be rearranged to $r_i = (e_i\alpha_i)/e_i(2\alpha_i - 1) - \alpha_i + 1)$ when the number of prey types (m) in equation (1) is set to 2. Black lines represent a case where selection is negatively frequency dependent; blue lines represent positive frequency dependence; red lines represent a case where the strength of selection is independent of environmental frequency and also a case where predators are killing prey in proportion to their relative abundance in the environment.

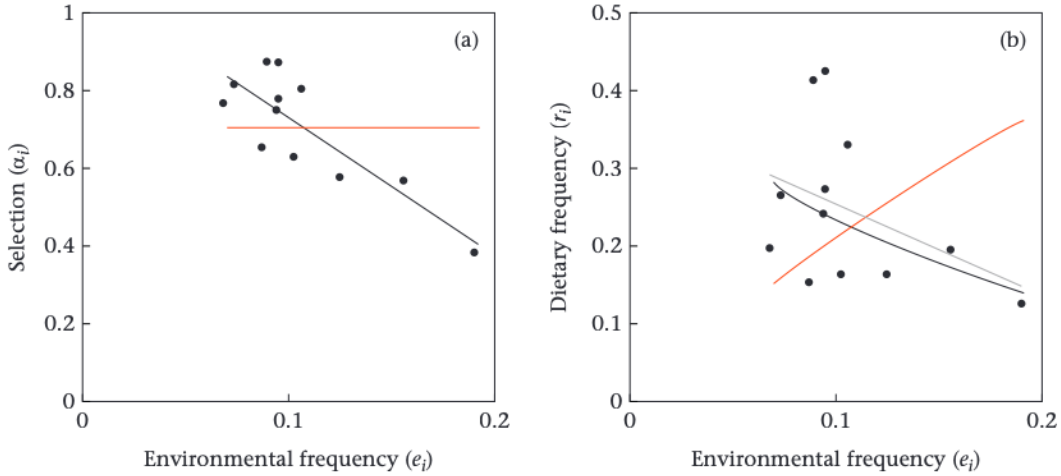

Figure A4. (a) The relationship between e_i and α_i and (b) the corresponding e_i and r_i relationship for wolves preying on senescent male elk in Yellowstone National Park. The black line in (a) represents the best-fitting model for the observed e_i and α_i data and suggests negatively frequency-dependent selection. In (b), the black line is the expected relationship between e_i and r_i when selection is negatively frequency dependent and directly corresponds to the black line in (a). The grey line in (b) represents the best-fitting model for the observed e_i and r_i data. The red lines represent a null hypothesis where selection is independent of environmental frequency. More precisely, the red line in (a) has slope = 0 and an intercept that is equal to the mean level of selection (α) observed over the study period for senescent male elk, such that it represents the null hypothesis where the overall strength of selection is similar to that observed empirically but it does not vary with environmental frequency. The red and black lines in (b) were calculated using the equation in Fig. A3.

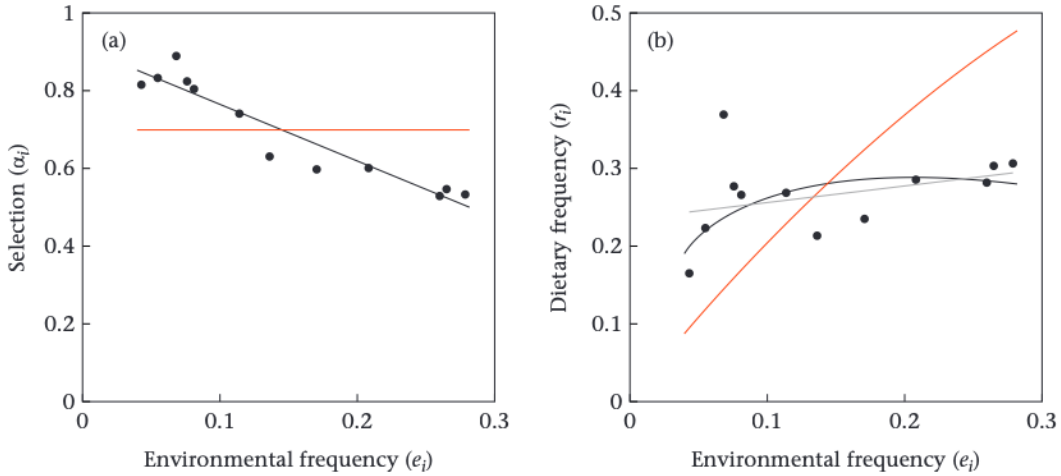

Figure A5. (a) The relationship between e_i and α_i and (b) the corresponding relationship between e_i and r_i for senescent female elk. All data and lines represent the same things as those described for male elk in Fig. A4, except they pertain to wolves preying on senescent female elk.

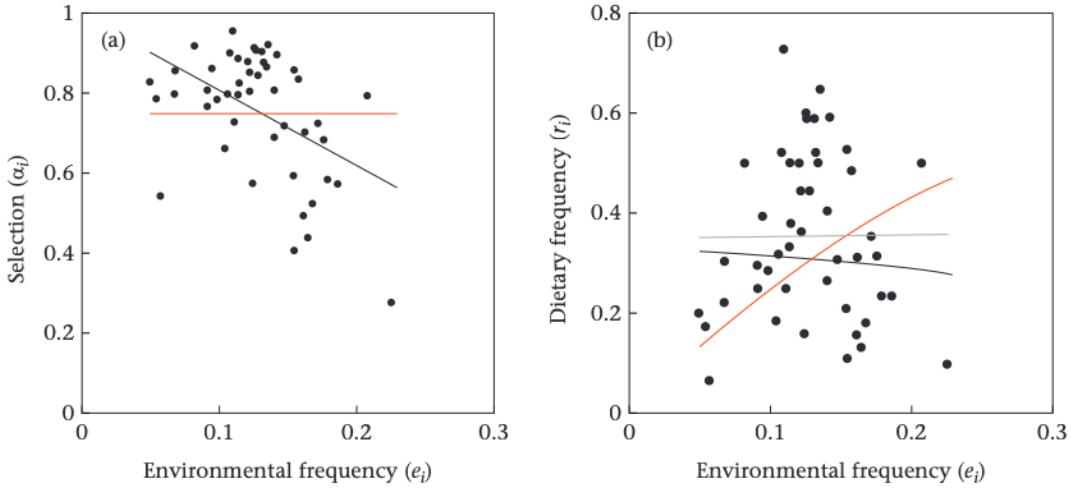

Figure A6. (a) The relationship between e_i and α_i and (b) the corresponding relationship between e_i and r_i for moose calves. All data and lines represent the same things as those described for male elk in Fig. A4, except they pertain to wolves preying on moose calves in Isle Royale National Park.

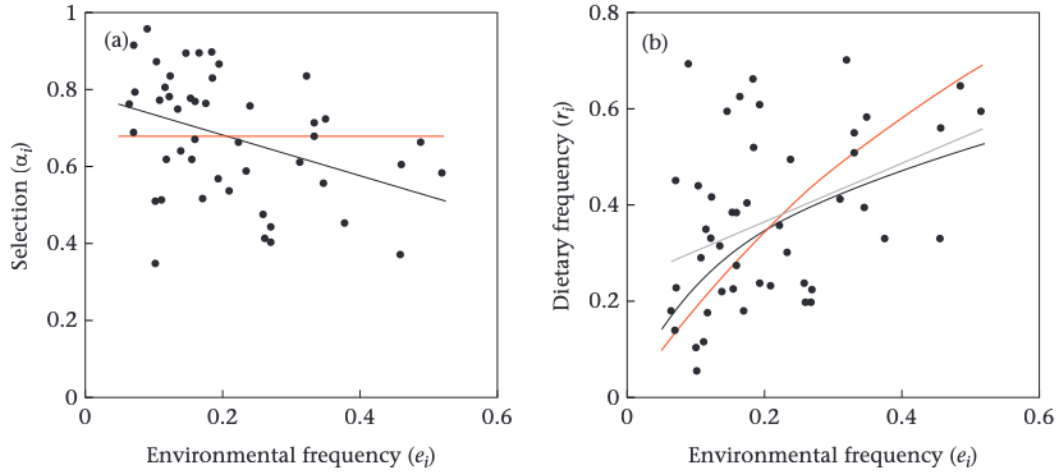

Figure A7. (a) The relationship between e_i and α_i and (b) the corresponding relationship between e_i and r_i for senescent moose. All data and lines represent the same things as those described for male elk in Fig. A4, except they pertain to wolves preying on senescent moose in Isle Royale National Park.

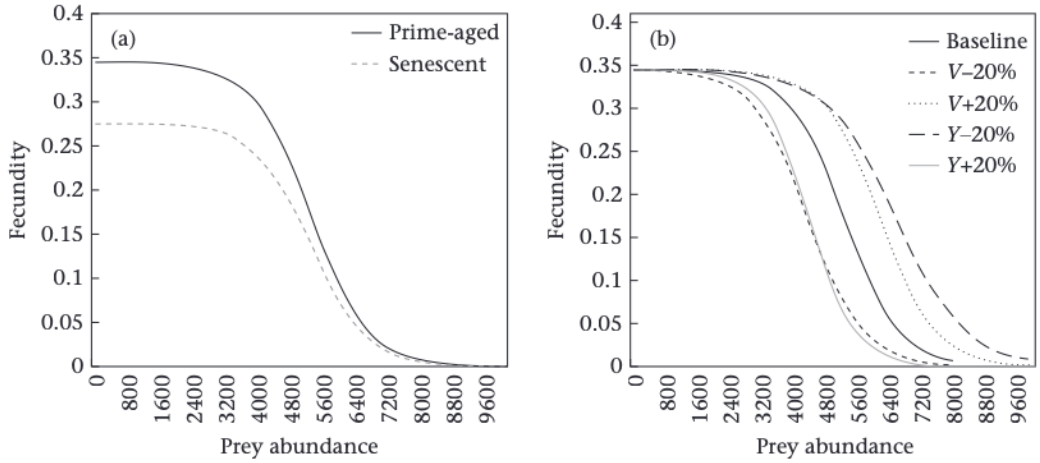

Figure A8. (a) Density-dependent fecundity used in the simulations for prime-aged and senescent prey. The strength and shape of density dependence is estimated from equation (A4). (b) Graphical depiction of how raising and lowering V and Y (in equation (A4)) by 20% affected the shape of the fecundity function in the sensitivity analysis (for details, see Appendix 2, Simulations and Sensitivity Analysis).

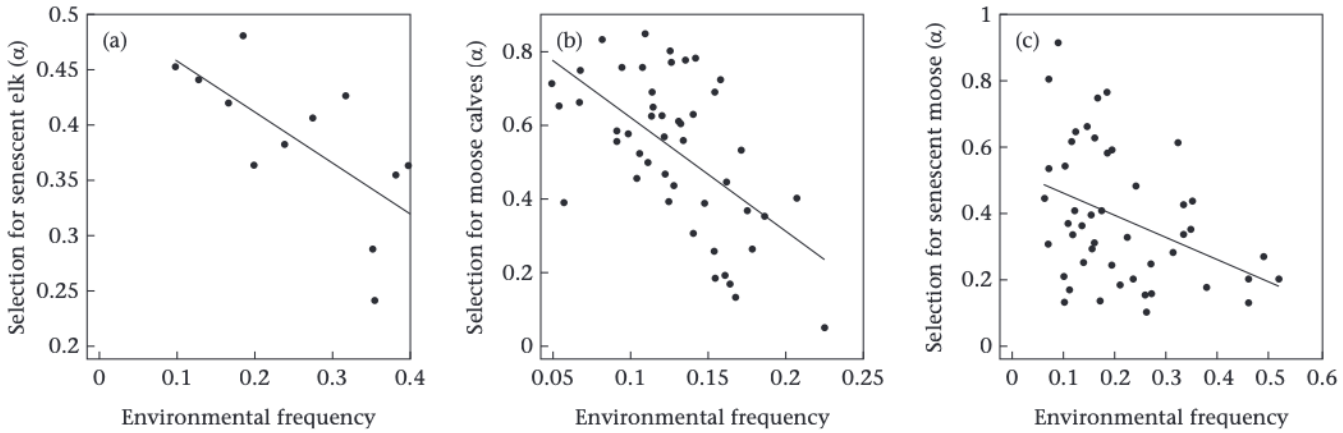

Figure A9. Frequency-dependent selection by predators used in the predator–prey simulation models. (a) Selection for senescent elk in the northern range of Yellowstone National Park, 1998–2009, when male and female elk were combined. (b, c) Selection for calves and senescent individuals in Isle Royale National Park. The data in (b) and (c) are the same as that depicted in Fig. 3 of the main manuscript. The lines in (a), (b) and (c) are equations (A15), (A16) and (A18), respectively, and are close linear approximates of the lines depicted in Figs 2 and 3.

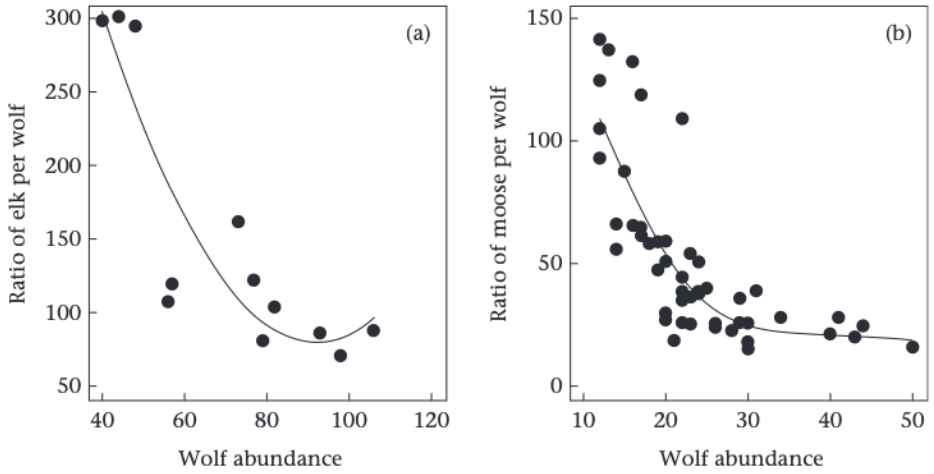

Figure A10. The ratio of prey (elk or moose) per predator (grey wolf) shown in relation to wolf abundance in (a) Yellowstone National Park and (b) Isle Royale National Park. Circles are annual estimates of the ratio of the primary prey species (an indicator of wolf per capita resources) per wolf in Yellowstone during 1998–2009 and Isle Royale during 1959–2007. In (a), the solid line represents fitted values from a second-order polynomial model that explained 76% of the variance in elk-to-wolf ratios. In (b), the solid line represents fitted values from a generalized additive model that explained 65% of the variance in moose-to-wolf ratios.

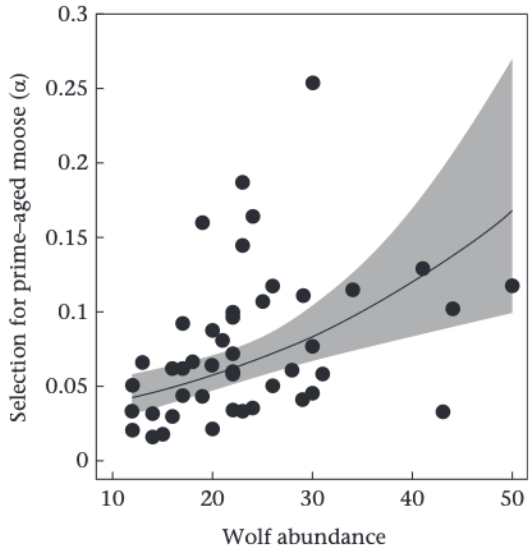

Figure A11. Selection for prime-aged moose (1–9 years old) by wolves in Isle Royale National Park shown in relation to wolf abundance. Circles are annual estimates of prey selection (α in equation 1 in main text) during 1959–2007. Solid lines are fitted values from a model predicting selection as a function of wolf abundance and grey areas indicate 95% confidence intervals around the fitted values.

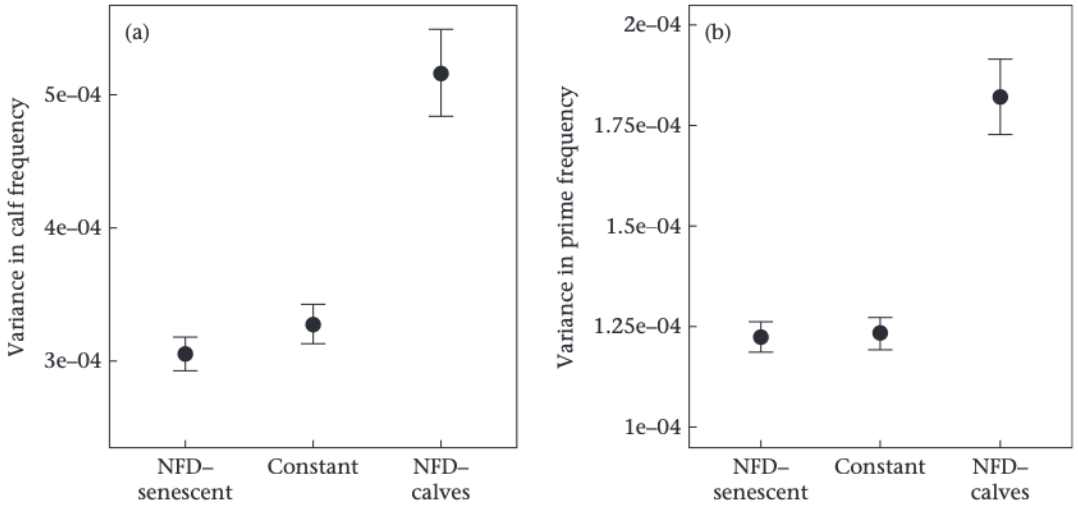

Figure A12. Results of simulations assessing the influence of frequency-dependent selective predation on variance of (a) the relative frequency of calves in the prey population and (b) the relative frequency of prime-aged adults in the prey population. Other details are as described in the legend for Fig. 4 of the main paper.